

2005

## Scanning probe microscopic characterization of flexible circuits

Vijayaraghava Nalladega  
*University of Dayton*

Follow this and additional works at: [https://ecommons.udayton.edu/graduate\\_theses](https://ecommons.udayton.edu/graduate_theses)

---

### Recommended Citation

Nalladega, Vijayaraghava, "Scanning probe microscopic characterization of flexible circuits" (2005).  
*Graduate Theses and Dissertations*. 4623.  
[https://ecommons.udayton.edu/graduate\\_theses/4623](https://ecommons.udayton.edu/graduate_theses/4623)

This Thesis is brought to you for free and open access by the Theses and Dissertations at eCommons. It has been accepted for inclusion in Graduate Theses and Dissertations by an authorized administrator of eCommons. For more information, please contact [mschlangen1@udayton.edu](mailto:mschlangen1@udayton.edu), [ecommons@udayton.edu](mailto:ecommons@udayton.edu).

SCANNING PROBE MICROSCOPIC CHARACTERIZATION  
OF FLEXIBLE CIRCUITS

Thesis

Submitted to

The School of Engineering of the  
UNIVERSITY OF DAYTON

In Partial Fulfillment of the Requirement for  
The Degree

Master of Science in Mechanical Engineering

By

Vijayaraghava Nalladega

UNIVERSITY OF DAYTON

Dayton, Ohio

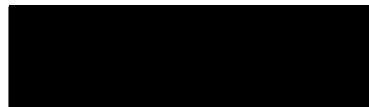
August 2005

## Scanning Probe Microscopic Characterization of Flexible Circuits

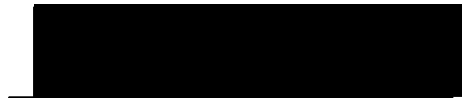
### APPROVED BY:



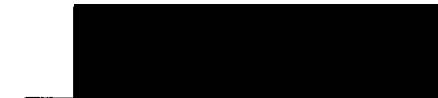
Shamachary Sathish, Ph.D.  
Advisory Committee Chairman  
Professor, Materials Engineering  
Department



Kevin Hallinan, Ph.D.  
Committee Member  
Chair, Mechanical & Aerospace  
Engineering Department



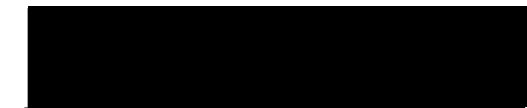
Vinod Jain, Ph.D.  
Committee Member  
Professor, Mechanical & Aerospace  
Engineering Department



Shankar Mall, Ph.D.  
Committee Member  
Professor, AFIT  
Wright-Patterson Air Force Base



Donald L. Moon, Ph.D.  
Associate Dean  
Graduate Engineering Programs and  
Research  
School of Engineering



Joseph Saliba, Ph.D., P.E.  
Dean, School of Engineering

## **ABSTRACT**

### **SCANNING PROBE MICROSCOPIC CHARACTERIZATION OF FLEXIBLE CIRCUITS**

Nalladega, Vijayaraghava  
University of Dayton 2005

Advisor: Dr. Shamachary Sathish

Flexible circuits have played an important role in miniaturization of the electronic components and devices. They provide pathway for carrying current to different parts of the components of devices. The flexibility provided by the flexible circuits has advanced major improvements in microelectronic industry. With the continued shrinkage of the size of the micro-electronic devices, the dimensions of interconnects are also shrinking. The current carrying capacity of the flexible circuit interconnects depend on the microstructure of the copper wire sandwiched between polymeric layers. The size reduction of the flexible circuits has led to new processes for laying the copper wire with very small grain sizes. The long-term reliability of the flexible circuit depends on the microstructure of the copper wire as well as the uniformity of the polymer-copper interface. With the continued shrinkage of the size of components and devices, the dimensions of the defects are reaching the resolution limit of many conventional quality-control instruments

and hence there is a need for newer techniques. This thesis presents application of combined techniques of Atomic Force Microscope and Ultrasonic Force Microscope, to investigate the microstructure of copper in flexible circuit with out necessity of removal of polymer layer, and the defects at the copper- polymer interface. The images obtained on the same regions of the samples using UFM were compared with that of the AFM images. The contrast in the Ultrasonic Force Microscopy shows grain structure of the copper wire as well as detailed features of defects at the polymer-copper interface. In majority of the samples the average grain size was found to be in the range of 100- 500 nm. On the other hand the delaminations of the size of a few tens of nanometers were observed. Experiments were conducted to study the growth and evolution of nano-delaminations, while passing a current through the flex circuit. The results and analysis of microstructure of copper in flex circuits from different manufactures are presented. The distribution of delaminations at different location in flex circuits is presented and their importance is discussed. The role of AFM and UFM as a possible quality control tool in microelectronics and computer industries is discussed.

## **ACKNOWLEDGEMENTS**

This study was supported by Seagate Technology Inc. and was carried out at Center for Materials Diagnostics (CMD), University of Dayton Research Institute (UDRI). I would like to thank Dr.Amarjit Brar of Seagate Technology for providing the samples required for this study. I would like to acknowledge the financial support provided by Graduate School, Department of Mechanical Engineering and Mr. Robert Andrews of Structural Integrity Division, UDRI. Thanks are also due to Mr.Yi Yang Tsai for training me on AFM instrument. I would like to thank my thesis committee members Dr. Kevin Hallinan, Dr. Vinod Jain and Dr. Shankar Mall for their suggestions and feedback on my thesis work.

Finally, I would like to express my sincere gratitude to my advisor Dr.Shamachary Sathish for his constant encouragement and motivation during the course of this project. His guidance during the project helped me to learn many new things and made this project a great learning experience.

## TABLE OF CONTENTS

Abstract .....	iii
Acknowledgements .....	v
List of Figures .....	ix
CHAPTER 1 INTRODUCTION	
1.1) Motivation .....	1
1.2) Flex Circuits .....	3
1.2.1) Background .....	3
1.2.2) Definition and Types of Flex Circuits .....	4
1.2.3) Reasons for use of Flex Circuits .....	7
1.2.4) Flex Circuit Materials .....	8
1.2.5) Flexible Circuit Manufacturing and Assembly .....	14
1.2.6) Testing of Flex Circuits .....	16
1.2.7) Applications of Flex Circuits .....	17
1.3) Flex Circuits in Hard Disk Drives .....	18
1.4) Importance of Microstructure .....	22
1.5) Effect of Defects at Copper-polymer Interface .....	24

## CHAPTER 2 INSTRUMENTATION AND EXPERIMENT

2.1)	Introduction .....	26
2.2)	Principle of AFM .....	27
2.3)	Instrumentation .....	28
2.4)	Modes of AFM .....	34
2.5)	Force Curves .....	35
2.6)	Tapping Mode AFM .....	38
2.7)	Ultrasonic Force Microscopy (UFM) .....	41
2.8)	Contrast Due to Elasticity at Nano-scale .....	43
2.9)	Experiment .....	49

## CHAPTER 3 MICROSTRUCTURAL ANALYSIS

3.1)	Importance of Microstructure .....	51
3.2)	Advantages of AFM-UFM in Microstructural Analysis .....	52
3.3)	Flex Circuit Samples Studied .....	53
3.4)	AFM-UFM Results .....	54
3.5)	Tapping Mode AFM Results .....	69
3.6)	Discussion of Microstructure Analysis Results .....	72

## CHAPTER 4 IN-SITU IMAGING OF GROWTH OF DELAMINATIONS

4.1)	Delaminations at Metal-Polymer Interface .....	74
4.2)	Results .....	76
4.3)	Discussion of the Results .....	83



## CHAPTER 5 CONCLUSIONS

5.1) Summary .....	87
References .....	91

## LIST OF FIGURES

1. Single- sided flex circuit construction .....	5
2. Double-sided flex circuit construction .....	6
3. Multilayer flexible circuit construction .....	6
4. Rigid flex multilayer flex circuit construction .....	7
5. Typical single-sided flex circuit manufacturing steps.....	15
6. Schematic diagram of roll-to-roll processing system .....	16
7. Schematic diagram of hard disk drive .....	19
8. Flex circuit in a hard disk drive .....	19
9. Schematic of a flex circuit used in a hard disk drive.....	21
10. Schematic of contact mode AFM .....	28
11. Schematic of AFM head .....	30
12. Piezo-electric tube scanner .....	30
13. Typical AFM and tapping AFM cantilever/tip dimensions .....	32
14. Typical force curve and the points along a force curve .....	36
15. Schematic of tapping mode AFM.....	39
16. Schematic of UFM .....	42
17. Tip –sample interaction modeled by Hertzian contact.....	44
18. A Rheological model for applying a displacement modulation to a transducer under a sample .....	46

19. Plot of frequency Vs. $d_1/z_1$ .....	47
20. An optical image of the flex circuit .....	55
21. AFM-UFM image of copper on sample #1 .....	55
22. AFM-UFM image of the same region with different frequency and scan size .....	56
23. Microstructure of copper on sample # 2 .....	58
24. Microstructure of copper on Sample # 2 at a different location on the same copper line .....	58
25. Microstructure of copper in sample # 3 .....	59
26. Microstructure of copper on sample # 3 obtained at a different region .....	60
27. Microstructure of copper in sample # 4 .....	60
28. Microstructure of copper of sample # 4 at a different region on the copper line .....	61
29. Optical image of the flex circuit sample # 5 .....	62
30. Microstructure of copper on sample # 5 on region 1 .....	63
31. Image obtained at region 2 of sample # 5 .....	63
32. Image obtained at region 1 of sample# 6 .....	64
33. Image obtained on region 2 of sample # 6 .....	64
34. Uniform microstructure of copper in sample # 7 (region 1).....	65
35. Microstructure of copper at region 2 of sample # 7 .....	66
36. Microstructure of copper on sample # 8 (region 1) .....	67
37. Microstructure of copper on sample # 8 (region 2).....	67
38. Uniform microstructure of copper in region 1 of sample # 9.....	68
39. Microstructure of copper at region 2 of sample # 9.....	69

40. Tapping Mode AFM image of copper on a flex circuit.....	70
41. Topographic and amplitude images (Tapping Mode AFM) on a flex circuit .....	71
42. Optical microscope image of the flex circuit after micro bonding.....	76
43. Defects in the polymer of the flex circuit .....	77
44. Growth of delaminations after two hours of 50 mA current.....	78
45. Image taken after 20 hours of passing the current (50mA).....	78
46. Image after 72 hours of 50 mA current.....	79
47. Image obtained after 160 hours.....	80
48. Image taken inside a delamination.....	81
49. Delaminations in region 2.....	82
50. Delaminations after 48 hours of passing 200 mA (region 2).....	82
51. Image taken after passing 800 mA current for 24 hours.....	83

## LIST OF TABLES

1. Comparison of selected properties of different flexible base films.....	10
2. Relative comparison rating of flexible electrical base films.....	12
3. Comparison of selected properties of flex circuit adhesives.....	13
4. Application areas of flex circuits.....	17

## **CHAPTER 1**

### **INTRODUCTION**

#### **1.1) Motivation**

The electronics industry is constantly moving towards the miniaturization of the electronic devices. Consequently, electronics interconnection packaging system, which is an important part of the microelectronic devices, has also undergone a remarkable change since its inception. The cost/performance improvements achieved in the field of packaging has been astounding. An analyst suggested [1] that if the commercial airline industry, which approximately began at the same time as electronics, had been able to keep pace with the cost/performance gains of electronics, we would today be flying in aircrafts that held thousands of passengers on journeys that took only few minutes to complete with ticket prices that would be less than a dollar. The above scenario sums up the amazing progress of the electronics industry which resulted in reduction of costs and high performance from the devices. This exceptional improvement is made possible by rapid progress and cutting edge technology in the filed of manufacturing. Flex circuit technology is the result of such advances in the process of manufacturing methods. Flexible circuit technology has opened a new era of opportunity to electronic package designers,

who were confined to two-dimensional world, allowing them the freedom of physical movement in three-dimensional space. Today, flex circuits are used in many diversified fields such as automotive, medical, military, computers, industrial controls, instruments etc.,

Even though the flexible circuit technology is becoming a first choice for numerous applications, it is not without its share of problems. Apart from small problems like processing of thin materials, cost there are reliability issues [1] which need to be addressed. Consequently, the conventional techniques which have been applied in the semiconductor industry for years for material characterization cannot be used effectively due to their relative lack of spatial resolution in comparison with the device dimensions. The introduction of scanning probe techniques has given the researchers, high resolution imaging tools which can image topography at atomic scale as well as an ability to image nano sized defects in the micro/nano level devices. The primary goal of this present study is to characterize the flex circuits using scanning probe techniques of Atomic Force Microscopy (AFM), Ultrasonic Force Microscopy (UFM) and Tapping mode AFM (TAFM). The microstructure of the copper film sandwiched between the polymer layers and the defects at the polymer copper interface are investigated. The microstructure of the copper films has been imaged through the polymer layer to determine the grain size variations. Polymer-copper interface was examined to study the process induced delaminations. In-situ study of the growth of delamination during flow of current through the circuit has been

performed to simulate the development of defects during the operation and usage of the flex circuit.

## **1.2) Flex Circuits**

### **1.2.1) Background**

Flexible circuits have been used in electrical/electronic applications since World War II. A flat conductor cabling resembling flex circuits was used in a number of different weapons systems. These were one key method of transmission of flexible interconnect technology. Patrick O Bryan, an engineer working for the Lockheed Company was among the first to recognize the potential of flex circuits. He has applied flexible wiring harness technology for numerous applications in the field of avionics. He also went on to find new applications for flex circuits such as automotive dash boards [1]. Today, flexible circuits are used in nearly every imaginable type of electrical and electronic product. They are one of the fastest growing interconnect product in the field of electronics. According to industry statistics, for the year 2000, flexible circuits represent an approximately \$ 5 billion dollar market worldwide with an anticipated growth rate of about 15% per year [1]. The following paragraphs will discuss about the flex circuits in detail.

### **1.2.2) Definition and Types of Flex Circuits**

According to Terms and Definitions for Printed Boards, a document published by the Institute for Interconnecting and Packaging Electronic Circuits, flexible circuit is defined as:

“A patterned arrangement of printed wiring utilizing flexible base materials with or without flexible cover layers”.

Flexible circuits can be fabricated in different forms. They have the same formats as rigid printed circuits but they can also be created in forms which will be inappropriate or impossible for rigid printed boards. A brief description of some of the types of flex circuits is given below.

#### **i) Single-sided Flex circuits:**

Single sided flexible circuits (Figure 1) are the most common type of flexible circuit produced and most often used and best suited to dynamic flex applications. They consist of a single conductor layer of either metal or conductive polymer on a flexible dielectric film with component termination features accessible from only one side. They can be made with or without a cover layer.



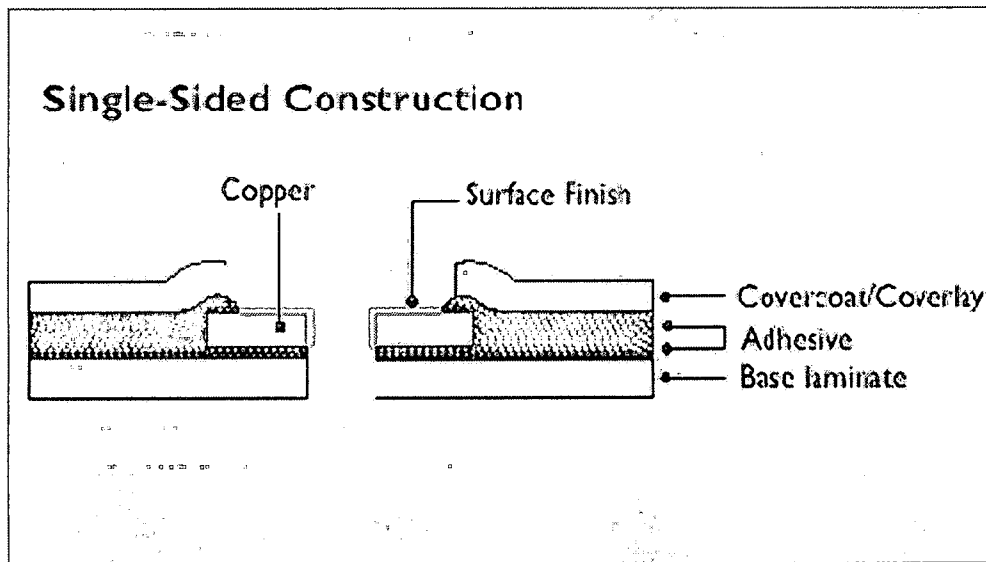


**Figure 1:** Single- sided flex circuit construction.

ii) Double Access Flex Circuits

These circuits have a single conductor layer but can be accessed from both sides. Such constructions have advantages but they are frequently more expensive than two metal layer flex alternatives. These circuits offer the advantage to the designer of allowing him to place components on both sides of the circuit.

iii) Double-sided Flex Circuits

These are flex circuits with two conductor layers (Figure 2). They can be fabricated with or without plated- through holes. Terminations for electronic components can easily be provided for on both sides of the circuit.

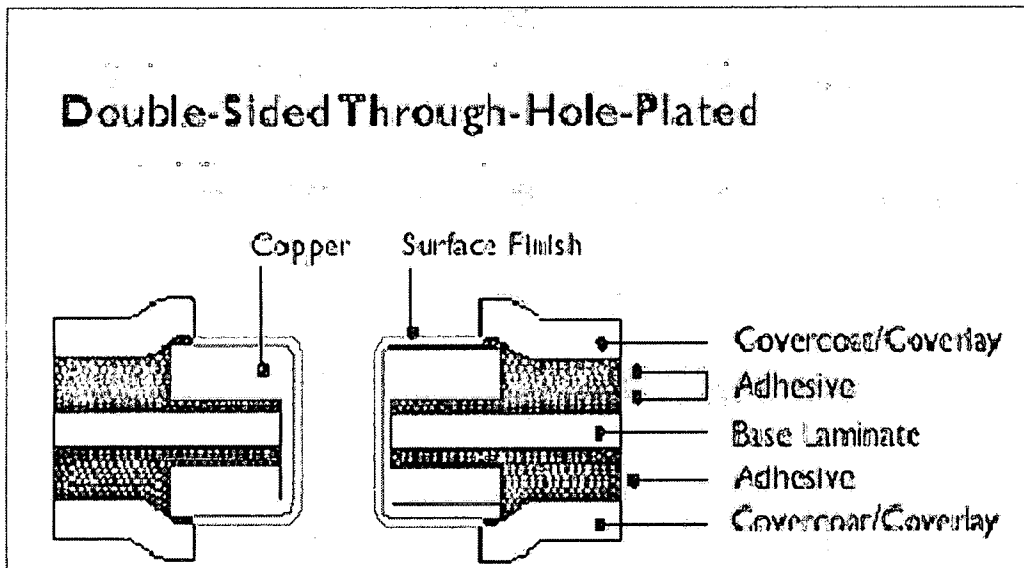


**Figure 2:** Double-sided flex circuit construction

iv) Multilayer Flex Circuits

Flex circuits with three or more layers of conductors interconnected by means of plated through holes are referred to as multilayer flex circuits (Figure 3).

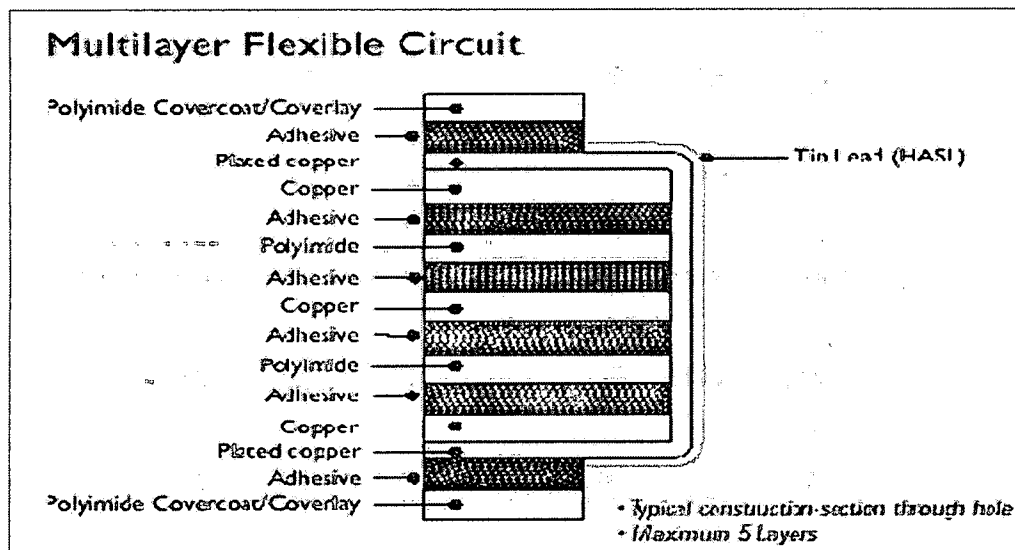


**Figure 3:** Multilayer flexible circuit construction

v) Rigid-flex circuits

Rigid-flex circuits (Figure 4) are a hybrid construction consisting of rigid and flexible substrates laminated together into a single package and electrically interconnected by means of plated-through holes. They are used where light weight, maximum integration and reliability are requirements. These flex circuits were initially used extensively in military applications and now they are also used in commercial applications such as laptop computers.

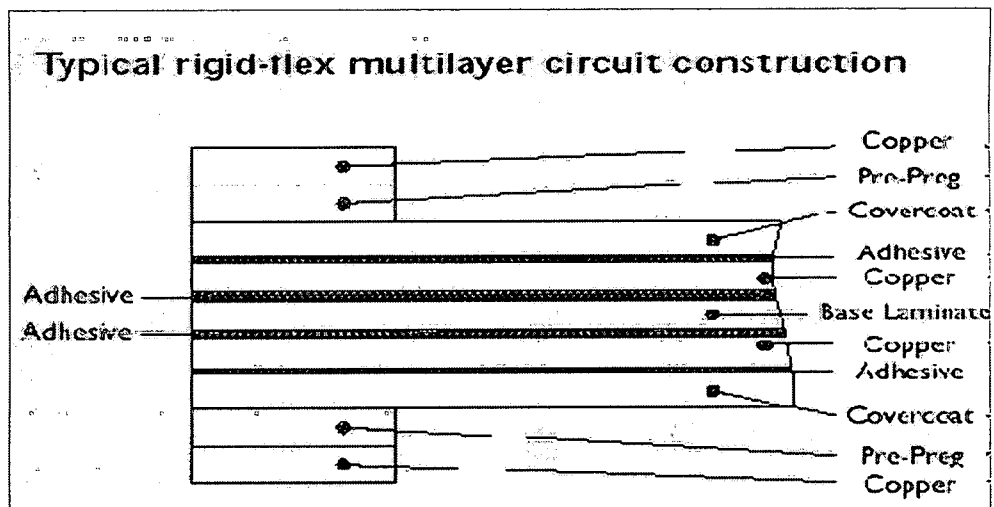


Figure 4: Rigid-flex multilayer flex circuit construction

### 1.2.3) Reasons for Use of Flexible Circuits

Many reasons exist for choosing flex circuits for an interconnection in electronic package. The solutions based on flexible circuits are often driven by the lack of viable alternatives. Some of the reasons for using flexible circuits are described below:

**Package size reduction:**

Flex circuits are among the thinnest dielectric substrates available for electronic interconnection packages. A total thickness of 0.002 in flex circuit can be produced.

**Weight reduction:**

Another important reason for using flex circuit is the weight reduction of an electronic package. Flex circuits can reduce the weight of a rigid printed circuit by almost 90%.

**Dynamic flexure of circuitry:**

The thinness of the material coupled with their ability to use thin copper foil makes flexible circuits the best candidates for dynamic flexible applications.

**Enhanced electrical properties:**

The materials used for flexible circuits are uniform in electrical properties. Flexible circuits are well suited to the manufacture of transmission line cables which must operate in the 40 to 60 ohms impedance range. In certain applications, flexible circuits have been used to reduce the inductance of a transmission line.

**1.2.4) Materials Used for Construction of Flex Circuits**

Wide variety of materials can be used as flexible substrates in the manufacture of flex circuits. However, there are some certain characteristics of the materials that can be used as a substrate in flex circuits. Those desirable characteristics include dimensional stability, thermal resistance; tear resistance,

good electrical properties, flexibility at temperature extremes, low moisture absorption, and chemical resistance. Apart from these characteristics, general concerns such as the availability, cost of the material should also be taken into account.

The basic elements in the construction of a flexible circuit are – a base material, adhesive and metal foil. Coverlayers are also used sometimes over the metal foil to encapsulate the circuitry and prevent bridging of the circuits during the soldering operation. Apart from that, a coverlayer also serves many important mechanical functions including enhancement of the flexural life of the finished product. Since the basic elements in the flex circuit are limited, it is obvious that all these materials are important in the reliable working of the final product.

#### **Flexible Base Materials:**

The base material is a flexible thin film that provides the foundation for a flexible laminate. The base material is used to identify the finished flexible circuit, e.g. polyimide or polyester flex circuit. The polymer which is used as the base material provides the bulk physical and dielectric properties required of the circuit. Even though there are many potential materials for use as base material for flex circuits, the number of qualified materials is currently quite limited. Polyimide and Polyester are two most commonly used base materials for flexible circuits. Table 1 gives a list of base materials used in flex circuit construction along with some of their properties. The choice of the particular base material is guided by the economics of the end-product, assembly technology needed for

the final product. A brief description of polyimide and polyester base materials is given in the following paragraphs.

**Table 1:** Comparison of selected properties of different flexible base films

Substrate	Dielectric Constant	Dielectric Strength (volts/mil)	Moisture Absorption (%)	Tensile Strength (psi)
Polyamide	2.0	380	3.0	11,000
Fluorinated ethylene-propylene	2.0-2.5	5000	<0.01	2-3,000
Polyetherimide	3.4	6200	1.2	15,000
Polyethylene	2.3	1300	<0.01	6,000
Polyester	3.2	7000	<0.08	25,000
Polyimide	3.5-4.0	2500-3200	1.3-3.0	35,000

**Polyimide:**

Polyimide is the most commonly used base material in the construction of the flexible circuit. These materials have excellent flexibility at all temperatures, good electrical properties, excellent chemical resistance, very good tear resistance but have poor tear propagation. These materials also have an added advantage of a coefficient of thermal expansion that matches that of copper, thus minimizing the effect of stress in the final product because of mismatch in the materials. Since polyimides can be chemically milled, unlimited number of unusual designs can be made in the finished product. Even though polyimide has many advantages, it also has disadvantages such as high moisture absorption (which can lead to serious reliability issues in real time usage of the product) and relatively high cost. Nevertheless, polyimide flex circuits have been most popular for military, medical and applications where dynamic flex action is needed.

**Polyester:**

These are used extensively in low-end flexible circuits and are commonly used in membrane switch applications and hand-held calculators. It is a lower temperature thermoplastic and can be easily heat formed into permanent shapes. The advantages of polyester include very low cost, good tear resistance, very good flexibility, good chemical resistance, low moisture absorption and good balance of electrical properties. But the downside of using the polyester is that it has very limited suitability for solder based assembly operations due to its low melting point. Also these materials are not well suited for extreme cold operations since they become brittle. Usually the service temperature for this material is in

the range of -60 ° C to 105° C. Using polyester in the situations where the tolerances are tight tend to become problematic to the manufacturer due to its dimensional instability.

**Table 2:** Relative comparison rating of flexible electrical base films

Base Material	Electrical Properties	Moisture Absorption	Dimensional Stability	Chemical Resistance	Flexibility
Polyester	↑	↑	↔	↑	↑
Polyimide	↑	↓	↑	↑	↑
Polyethylene naphthalate	↑	↑	↔	↑	↑
Epoxy composites	↔	↑	↑	↑	↓
Fluoroplastics	↑	↑	↓	↑	↑
Aramid paper	↔	↓	↔	↑	↓
Good ↑ Fair ↔ Poor ↓					

### Adhesives

Adhesives are used to bond the metal foil to the base film in a flex circuit. They are also combined with base films to create coverlayer films. An adhesive plays an important role in the overall performance of the flex circuit. Often times, it is the adhesive which is the limiting element in the thermal performance of the flexible base laminate, especially if polyimide is used as a base material. Again,



as in the case of base materials, there are wide ranges of materials that can be used as adhesives. The most commonly used adhesives are polyester, epoxy and polyimide. The following table summarizes properties of different adhesives used in flexible circuit construction.

**Table 3:** Comparison of selected properties of flex circuit adhesives

Adhesive Type	Peel Strength post solder (min) (lb/in)	Adhesive Flow mils	Moisture Absorption (max.) (%)	Surface Resistivity (min. MΩ)	Dielectric Constant (@ 1MHz) (Max)
Polyester	N/A *	10	2.0	10 <sup>4</sup>	4.0
Acrylic	7.0	5	6.0	10 <sup>5</sup>	4.0
Epoxy	8.0	5	4.0	10 <sup>4</sup>	4.0
Polyimide (1)	5-12	5	1.0-2.0	10 <sup>5</sup>	3.3
Polyimide (2)	5	5	3.0	10 <sup>5</sup>	4.0
Butyrol:Phenolic	5	5	2.0	10 <sup>4</sup>	3.0

\*Because polyester is considered unsuitable for soldering the requirement does not apply

### **Metal Foils**

The conductive element of the flex circuit is provided by the metal foil. It is from the metal foils that the circuit paths are normally etched. Aluminum and copper are two most commonly used metals in the construction of flex circuits.

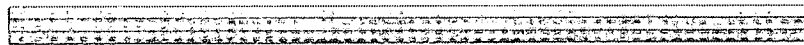
Copper is increasingly used as an interconnect metal in microelectronic devices due to its high conductivity, low resistivity, and high resistance to electro migration. Also copper has low values of RC delay. High values of RC delay, which are characteristic of Aluminum, are unacceptable because it decreases the speed of the devices. RC delay can be reduced by reducing either resistivity or by increasing the cross section of interconnections. Increasing of cross section is not appealing hence a lower resistivity metal is to be used instead of aluminum. Copper with its lower values of RC delay is an ideal candidate as interconnect metal. In spite of having so many advantages, copper does have some disadvantages especially when used in silicon based devices. Those are a) high diffusivity in silicon, b) poor adhesion to  $\text{SiO}_2$  and c) reactivity with environment. To overcome this problem, copper has to be passivated using a layer of polymer on that before it can be used in those devices. A standard electrodeposited (ED) copper is commonly used for static applications due to its columnar grain structure; while heat treated electrodeposited copper is used in dynamic flexing applications because of its recrystallised grain structure.

#### **1.2.5) Flexible Circuit Manufacturing and Assembly**

Many different methods have been used to fabricate and assemble the flex circuits. The choice of a particular manufacturing process depends on the complexity of the design and on the method of fabrication chosen. A few processing steps are required to manufacture single layer flex circuits, while it requires a number of processing steps and manufacturing methods like imaging,

plating, etching, drilling, lamination and several other methods for a complex flex products like rigid-flex circuits. Figure 5 illustrates typical steps for manufacturing of a single-sided flex circuit.

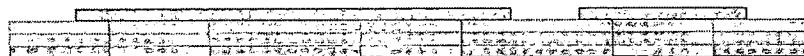
**Typical single-sided flex circuit manufacturing steps**



Flex circuit base material cut to size



Holes are drilled or punched into laminate



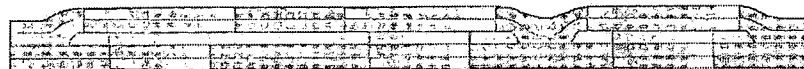
Etch resistant circuit pattern image is applied



Unprotected copper is etched away



Etch resist is stripped from the circuits



Prepunched coverlayer is laminated to the circuits

**Figure 5:** Typical single-sided flex circuit manufacturing steps

Different methods of manufacturing of the flex circuits are roll-to-roll processing, die cut imaging process, laser machining, electrolytic plate-up processing, etc.,

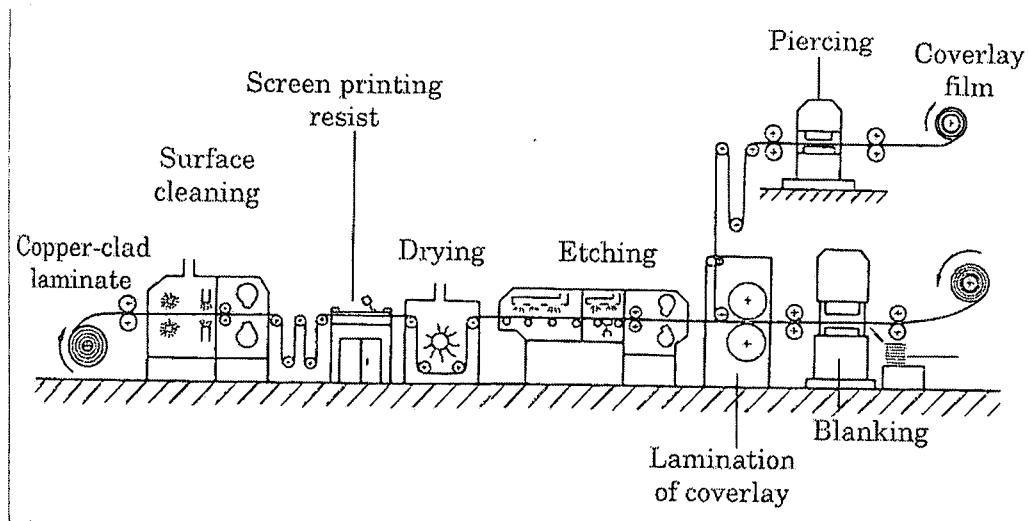


**Figure 6:** Schematic diagram of roll-to-roll processing system.

### 1.2.6) Testing of Flex Circuits

Inspection and testing of the flex circuits is a vital for the reliability of the product. Testing of the flex circuits is done in two stages. The first stage is the testing of the raw materials used for the manufacturing of the flex circuit, while in the second stage testing is performed on the finished product before it is put into use. The raw material is tested for physical, dimensional, chemical and environmental properties. Likewise, the finished flex circuit is also tested for physical, dimensional, environmental, electrical, solderability, construction integrity and cleanliness. Even though the testing done on the flex circuits assures some reliability, the reliability of the product when it is in real time use is not known. Some process induced defects may be known only when the product is in use. For example, air trapped in between the layers of polymer and metal and delaminations because of moisture absorption may not be seen until the real use. The present study addresses the issue of reliability of these flex circuits

when they are used in real time. This is simulated by passing current through the circuit and imaging the defect growth or delaminations, if they are present in the circuit, using AFM/UFM.

### **1.2.7) Applications of Flex Circuits**

Flexible circuit technology is the key enabler for making electronics lighter, faster, smaller, thinner, cheaper and more reliable. Flex circuits are used to interconnect electronic products that must be dynamically flexed from thousands to millions of times during their life time. They are also used in electronic packaging applications where flexing of the circuits is needed. Thus many application areas exist for the use of flex circuits in electronics industry (Table 4). Flex circuits are used in many applications covering all the basic markets for electronic products.

**Table 4:** Application areas of flex circuits

<b>Automotive</b>	<b>Computers</b>
-Instrument panel	-Dot matrix printheads
-Under bonnet controls	-Disk drive heads
-Headliner circuits	-Transmission line cable
-ABS systems	-Ink jet print heads
<b>Consumer</b>	<b>Industrial Controls</b>
-35 mm cameras	-Laser measuring
-Video cameras	-Inductor coil pick-ups
-Exercise Monitors	-Copying machines
-Hand held calculators	-Heater coils

**Medical**

- Hearing aids
- Heart pace-makers
- Defibrillators
- Ultrasound probe heads

**Military and Aerospace**

- Satellites
- Instrumentation panels
- Radar systems
- Jet engine controls
- Night vision systems
- Plasma displays

**Instruments**

- NMR analyzers
- X-ray equipment
- Particle counters
- Infra-red analyzers

**Miscellaneous**

- Smart weapons
- Laser gyroscopes
- Torpedoes
- Electronic shielding
- Surveillance systems
- Radio communication

**1.3) Flex Circuits in Hard Disk Drives**

Hard disk drives are magnetic storage devices used to read/write data in a computer [2]. A schematic diagram of a hard disk drive along with its parts is shown in the figure 7.

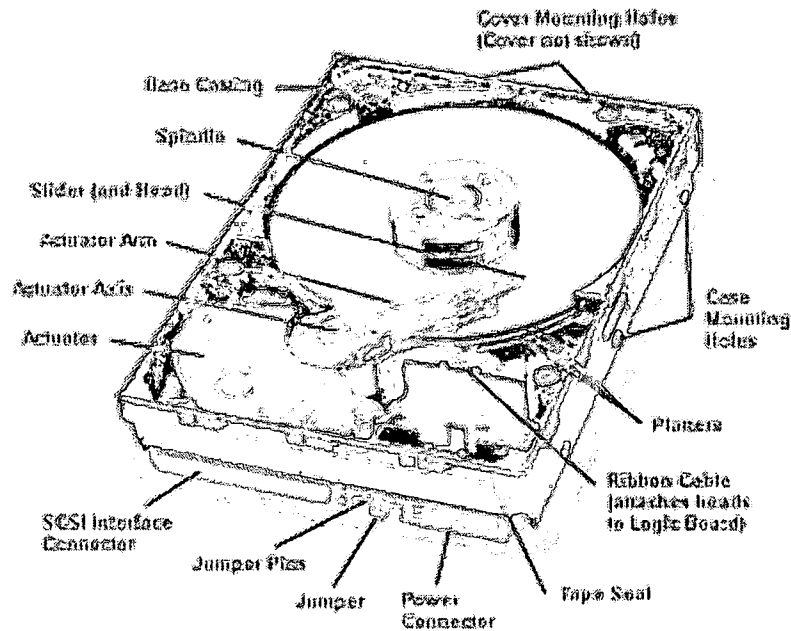


**Figure 7:** Schematic diagram of hard disk drive

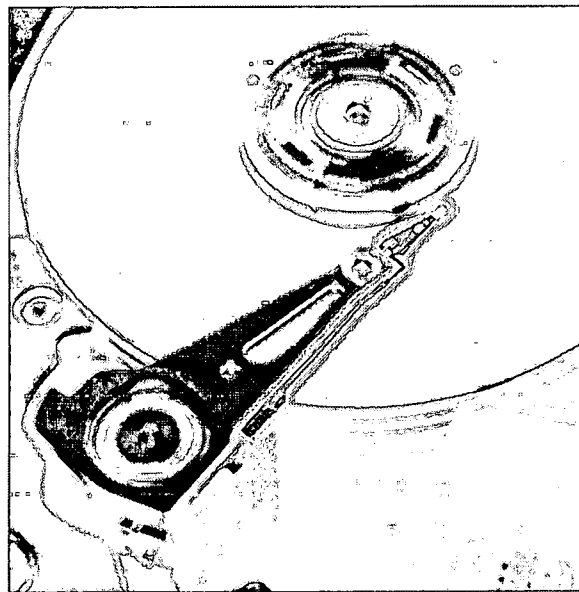


**Figure 8:** Flex circuit in a hard disk drive

A hard disk uses round flat disks called platters, coated with magnetic material which stores information in the form of magnetic patterns. The stack of the platters are mounted onto a spindle which rotate at high speeds (usually

4500 rpm), driven by a spindle motor connected to the spindle. To record or read information on/from the disk, electromagnetic read/write head sliders are used. The read/write head slider is mounted onto an arm which is mechanically connected into a single assembly and positioned over the surface of the disk by an actuator. A logic board controls the activity of the other components and communicates with the rest of the computer. Each hard disk platter has two surfaces one on each side of the platter. There is normally one head for each surface of the platter. Since most hard disks have one to four platters, most hard disks have two to eight read/write heads. Only one head can read from or write to the hard disk at a given time. The head slider floats over the disk and records the magnetic data onto the magnetic platters without ever touching the platter. The amount of the space between the head and the platter is called floating height. Usually, this floating height is about 0.5 micro inches. Flex circuits are used in two places in hard disk drives. One is to connect the stationary electronic components of the hard disk drive to the rotating arm which carries the read/write heads and the other is used on the arm of the hard disk to make an interconnection to the read/write heads (Figure 8). The choice of a flex circuit to connect the rotating arm to the electronic component is an obvious since the arm rotates millions of times during the life time of the hard disk and flex circuits are ideal for this kind of dynamic flexing action. A schematic of the flex circuit used in the hard disk drives is shown in figure 9.



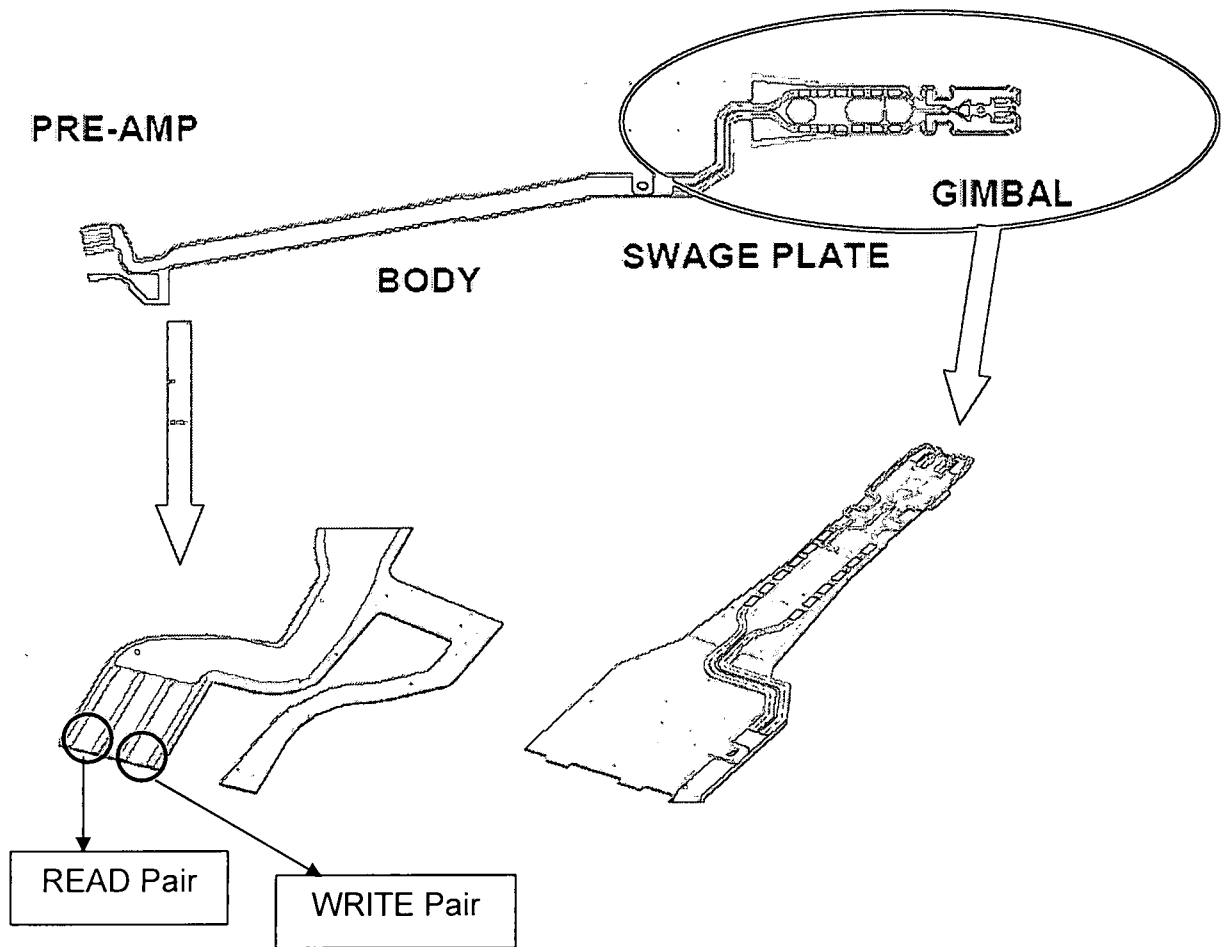


**Figure 9:** Schematic of a flex circuit used in a hard disk drive

The different components of a flex circuit used in a hard disk drive are shown in the figure. Gimbal assembly is the head slider assembly which is soldered on to the right end of the flex circuit and which is responsible for reading/writing of the data in the hard disk. Signals are transmitted between Pre-amp and the Gimbal assembly by means by two pairs of read and write copper lines which extend throughout the length of the flex circuit [3]. Microstructural variations and presence of defects in the region where the head slider is soldered, will affect the reliability of the system. Hence imaging the

microstructure and the defects in the region becomes important to assess the reliability of the system.

#### **1.4) Importance of Microstructure**

Microstructure of a material covers the scale of structural phenomena namely grains, particle sizes, dislocation densities, micro-cracking etc. Many of the properties of the engineering materials are directly and sensitively related to the microstructural features of the material. The microstructure of a material is determined by the processing technique used to manufacture the material and the properties are determined by the microstructure. This includes not only grains and particles but also various defects in the microstructure like porosity, microcrack and unwanted inclusions. Since the properties of a material are dependent on the microstructure, the study of microstructure can reveal a direct causal relationship between a particular microstructural feature and a specific property. The properties which are structure sensitive are yield strength, dislocation density, thermal conductivity, electrical resistivity.

Copper is increasingly becoming a metal of choice as interconnect in microelectronic devices [4]. As the size of the microelectronic devices are getting smaller, the study of microstructure of the copper interconnects is more crucial for the performance and the reliability of the device. A failure of one interconnect out of millions of submicron circuits can destroy the whole device. The failure mechanism can be known by studying the microstructure of the material. Also,

previous studies [5-7] have shown strong dependence of microstructure of copper in its resistance of electromigration. Thus microstructure is an important factor in assessing the reliability of the components used in microelectronic devices.

The microstructure of copper in flex circuits is also used as a quality control factor in hard disk drive industry. A flex circuit is used in a hard disk drive to connect the stationary electronic components to the read/write arm of the hard disk [1]. Grain size and grain orientation are the two important parameters which are utilized to study the quality of the flex circuits. The flex circuit with a favorable grain size and orientation is used in hard disks. Many techniques are used to image microstructure of the copper in interconnects. Some of them are Transmission Electron Microscopy, Electron Backscatter Diffraction, and X-ray micro-diffraction [8, 9]. These techniques are suitable to examine unpassivated free surfaces of copper. Moreover these methods require extensive sample preparation, time consuming, labor intensive as well as expensive. In many situations, when hard disc manufacturers acquire flex circuits from different vendors and need to perform evaluation of the microstructure of the copper film, the techniques of Transmission Electron Microscopy, Electron Backscatter Diffraction cannot be used without the removal of the polymer layer. High energy x-rays [10, 11] can penetrate through the polymer layer but the resolution of the technique may not allow visualization of individual grains. Thus there is a need for a high resolution imaging technique, which can image the copper through the polymer without having to remove it. In this study, the feasibility of using a

combination of AFM/UFM to image the microstructure of the copper through a polymer layer is examined.

### **1.5) Effect of Defects at Copper-polymer Interface**

The process of manufacturing of flex circuits involves lamination of copper film between polymer layers in presence of adhesives. During the process of lamination due to lack of adhesion between polymer and copper as well as polymer and polymer delaminations can occur. Also during the lamination process, absorption of excess moisture, or release of gases can lead to formation of voids both at the interfaces as well as in the polymer. Large delaminations can be identified and the component can be eliminated during quality control. With rapid advances in the field of microelectronic devices, the size of the devices is increasingly becoming smaller and the presence of defects, which are approaching the size of the devices, even on a nano scale will adversely affect the functioning and reliability of the devices. The presence of delaminations, voids, entrapped moisture can lead to several problems. One of the major problems is if the delamination occurs around a hole designed for soldering. During soldering operation the liquid metal is wicked into the delamination regions causing problems. While large delaminations can be identified it is difficult to detect small regions when they are of the dimension of the resolution limit of the instrument used for quality control. In certain situations the presence of defects like voids in the polymer, or delamination at the polymer

metal interface may grow to larger dimensions during the use of the flex circuit. These defects are expected to be life limiting factors in the use of flex circuits. In the last decade optical microscopy, Scanning Acoustic Microscopy, Scanning Kelvin Probe Microscopy, X-ray Photo-electron Spectroscopy have been used to investigate metal polymer interface [12-16]. These studies have addressed electrochemical interaction at the polymer metal interface. This thesis, apart from presenting investigation of the microstructure of copper, also describes study of defects in the polymer and polymer-copper interface using AFM and UFM. Defects developed during manufacturing have been examined in as received flex circuits. To study the defects developed during use of components, in-situ examination has been performed while passing a current through the circuit. AFM and UFM images were acquired while passing a current through the circuit at several intervals of time. Both defect initiation and growth of delamination is investigated.

## **CHAPTER 2**

### **INSTRUMENTATION AND EXPERIMENT**

A Digital Instruments Dimension 3000 Nanoscope IIIa AFM [17] has been used to characterize surface topography. To modify this instrument into an Ultrasonic Force Microscope, ultrasonic waves were propagated through the sample and measure the surface displacements thus facilitating to examine the elastic properties of the sample surface on nano-scale.

#### **2.1) Introduction**

The invention of Scanning Tunneling Microscope (STM), in 1981, by Binnig and his colleagues at the IBM Zurich laboratory has made possible obtaining of 3-D images of solid surfaces with atomic resolution. For this invention Binnig and Rohrer were awarded Nobel Prize in physics in 1986. The STM utilizes, tunneling current between an atomically sharp-tip and a sample to produce images with atomic resolution. The major drawback of the STM is that it can be used only with sample surfaces that are electrically conductive. The development of Atomic Force Microscope (AFM) [18] by Binnig, Quate and Gerber in 1985 not only overcame the limitation of STM but led to the new world of imaging with near atomic resolution of many physical properties of materials.

depend on tunneling of electrons, all surfaces can be imaged. Since its development, AFM has become a popular surface profiler for topographic and force measurements on micro to nano scale with atomic resolution. AFM can be used in any environment such as ambient air, various gases, liquid, vacuum, at low temperatures and high temperatures.

## **2.2) Principle of AFM**

Basic principle of AFM is shown schematically in Figure 10. It utilizes a sharp tip, 20-30 nm in radius and height 10-20 $\mu$ m, usually made of Si<sub>3</sub>N<sub>4</sub> attached to the end of a soft cantilever (100 $\mu$ m long). When the tip-cantilever is raster scanned across the sample surface, the cantilever moves up and down to follow the surface topography variation. Up and down movement of the cantilever is measured using an optical method. A beam of light from a laser source is reflected off the back of the cantilever. The up and down motion of the cantilever results in the deflection of the laser beam and it is measured by a position sensitive detector consisting of two closely spaced photodiodes whose output is further amplified and measured. The optical detection allows measurement of deflection of nearly 0.02 nm. The cantilever deflection is a direct measure of the interaction force between the tip and the sample surface. To obtain topographic information, the interaction force is used as a control parameter for a feedback circuit that maintains the force at a constant value by adjusting the sample Z position. The lateral resolution of AFM depends on the

diameter of the tip and by manufacturing smaller and sharper tips, the resolution can be increased. Topographic images with a vertical resolution of less than 0.1 nm and a lateral resolution of about 0.2nm have been obtained using AFM.

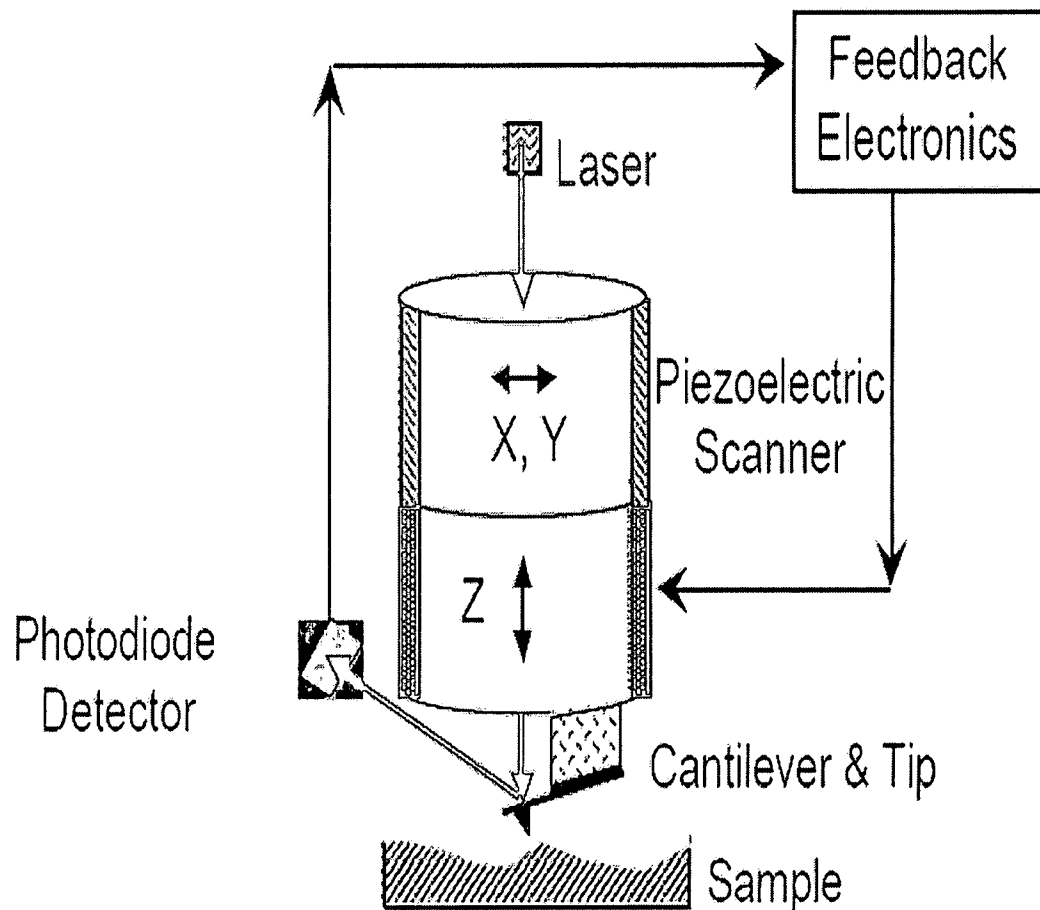


**Figure 10:** Schematic of contact mode AFM.

### 2.3) Instrumentation:

The Atomic Force Microscope consists of five basic components. They are

- i) Piezo-electric scanner to move the probe relative to the sample
- ii) A sharp tip mounted on a soft cantilever



- iii) A detection system for measuring the deflection of the cantilever and
- iv) A feedback control system to keep the deflection constant
- v) A computer to store and display the image

A short description of each component [19] is provided in the following paragraphs.

#### **AFM Scanner:**

AFM uses a piezo-electric scanner to scan the tip across the surface. The most commonly used scanner is tube scanner (figure 12). They are widely used in AFM due to their simplicity and their compactness. The scanner is constructed by combining independently operated piezo electrodes for X, Y and Z into a single tube, forming a scanner which manipulates samples and probes with extreme precision in 3 dimensions. AFM systems can have the scanners installed in the AFM head (figure 11) or below the sample stage. Depending on the scanner location, either the sample or the probe head will be raster scanned during the imaging. In the AFM system used for this experiment, the scanner is located in the AFM head and the sample is held stationary.

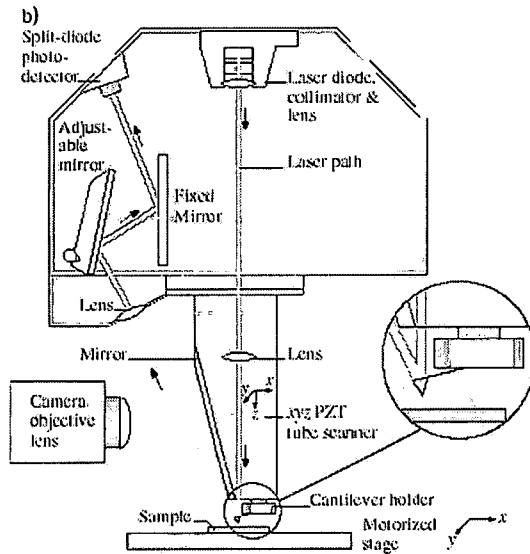


**Figure 11:** Schematic of AFM head

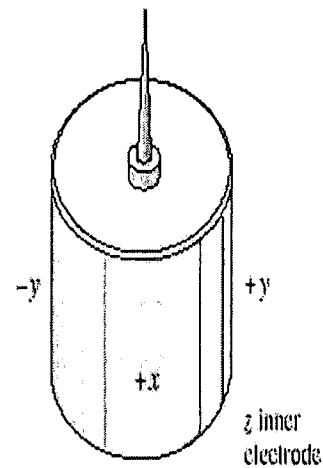


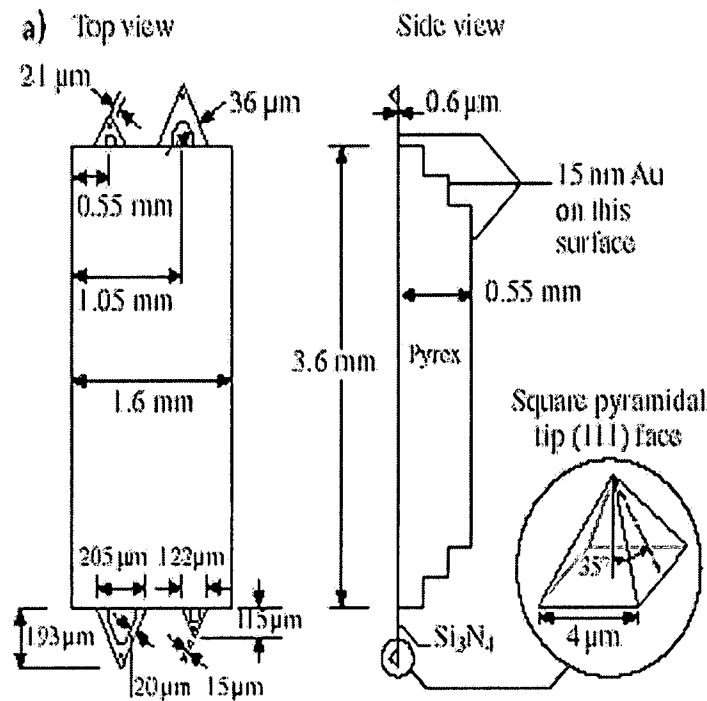
**Figure12:** Piezo-electric tube scanner

#### Probes:

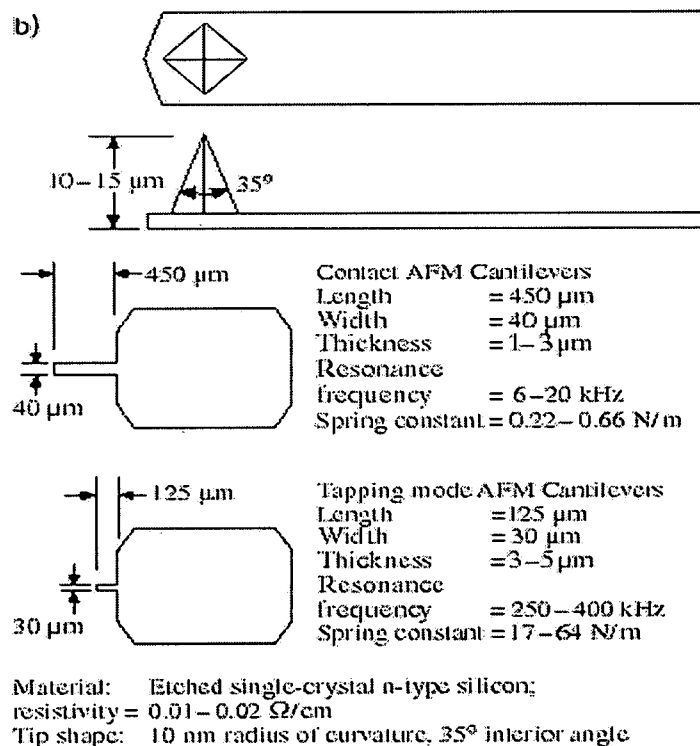
The key element in the AFM is the probe (cantilever and tip) which acts as force sensors. The probe in AFM should meet the following requirements: 1) low normal spring constant, 2) a high resonant frequency, 3) high lateral spring constant, 4) short cantilever length, and 5) a sharp tip. In order to register a measurable deflection with small forces, the cantilever must flex with a relatively low force requiring vertical spring constants of  $10^{-2}$  to  $10^2$  N/m for atomic resolution. The data rate or imaging rate in AFM is limited by the mechanical resonant frequency of the cantilever. To achieve a larger imaging bandwidth, the cantilever in AFM should have a high resonant frequency, around 30-100 KHz so that the cantilever is the least sensitive part of the system. Since the lateral forces cause lateral bending of the cantilever, high lateral spring constant in the cantilever is desirable to reduce the effects of lateral forces. A sharp protruding tip must be formed at the end of the cantilever to provide a well defined

interaction with sample over a small area. The tip radius must be smaller than the radii of corrugations in the samples in order for these to be measured accurately. Typically, the average radius of an AFM tip is around 20-30 nm.

Wide ranges of materials have been used for design and construction of the AFM probes. The most commonly used materials are  $\text{Si}_3\text{N}_4$ , Si and diamond. A schematic diagram of the most often used probes manufactured from silicon nitride cantilever, silicon cantilever are shown in figure 13.



Silicon Nitride AFM Tips



### Silicon Tips

**Figure 13:** Typical AFM and tapping AFM cantilever/tip dimensions

Silicon Nitride cantilevers are the most frequently used and are less expensive than other materials. They are very rugged and are suitable for imaging in any environments. The AFM instrument used in this experiment has a micro fabricated silicon nitride triangular cantilever with integrated square pyramidal tips made of plasma enhanced chemical vapor deposition using photolithographic techniques. Figure (a) shows four cantilevers with different sizes and spring constants on each cantilever substrate made of boron silicate glass. Only one cantilever is selected for a measurement. The spring constant of the tip used in our experiment was 0.12 N/m.

**Deflection Detection System:**

The forces acting on the tip of the AFM causes a cantilever deflection which can be measured by tunneling, capacitive or optical detectors. The most commonly used cantilever deflection system is the optical lever system. This method, also known as Beam Deflection Detection method is the deflection system used in the system used in the present instrument. In this method, a laser beam is reflected off a mirror and projected to a receiving target. Any change in the angular position of the mirror will change the position where the light ray hits the target. A photo diode segmented into four closely spaced devices detects the orientation of the end of the cantilever. Initially, the laser beam is set to hit the photodiodes in the middle of the two sub-diodes. Any deflection of the cantilever will cause an imbalance of the number of photons reaching the two halves. Hence the electrical currents in the photodiodes will be unbalanced. The difference signal is further amplified and used as input signal for feedback control.

**Feedback Control:**

A feedback control system is used in the AFM to keep the cantilever deflection constant. By measuring the difference signal in the photodiode quadrants, the amount of deflection can be correlated with a height. The feedback mechanism employed in the system enable the piezo-electric scanners to maintain the tip at a constant force (to obtain height information), or constant height (to obtain force information) above the sample surface. In constant force mode, as the tip is raster-scanned across the surface, the piezo will adjust the tip-sample separation so that a constant deflection set point is maintained. If

there is surface asperity in the path of the tip as it scans the surface, the cantilever deflection will increase and the feedback electronics will move the z height of the scanner to make the cantilever deflection back to the present point.

## **2.4) Modes of AFM**

The AFM can be operated in three modes viz., Contact, Non-Contact and Tapping (Intermittent contact) Mode. In contact mode, which is most commonly used mode in AFM, the tip is in constant contact with the sample surface. The principles and the instrumentation of the contact mode AFM was described in the preceding sections. The advantages of the contact mode AFM are high scan speeds, high resolution images and the ability to scan and image rough samples.. The excessive lateral forces on the sample surface during the scanning may damage softer samples due to the continuous contact of the tip with the sample. Thus this mode may not be useful for very soft samples like biological materials.

Non-contact mode AFM was introduced to use in situations where the tip contact may affect the sample surface in a subtle way. In this method, the tip is placed 50-150 Å above the sample surface and the attractive Vander Waals forces between the tip and the sample surface are detected. Since the attractive forces from the sample are substantially weaker than the forces used by contact mode, the tip must be given a small oscillation so that AC detection methods can

be used to detect the small forces between the tip and the sample by measuring the change in amplitude, phase, or frequency of the oscillating cantilever in response to force gradients from the sample. There is no damage to the samples in this case since there is no contact of the tip with the sample surface. But lower lateral resolution and slower scan speeds limit the usage of the non-contact mode AFM for most applications.

Tapping mode AFM is used to image samples that are very soft or easily damaged by continuous contact with tip. In this mode, the tip is intermittently in contact with the sample at each point and then lifting the tip off the sample surface to avoid dragging of the tip across the surface. A detailed explanation of tapping mode AFM will be given in subsequent sections. In experiments presented in this thesis, both contact and tapping mode AFM were used.

## **2.5) Force Curves:**

Force curve [20] is a plot of the force between the tip and the sample as their distance is changed. This is the most important feature in an atomic force microscope. Many of the features in the images as well as modification of AFM to image other physical properties other than topography depend upon an understanding of the force distance curve. Optimizing the force acting on the tip becomes essential to obtain good quality images. The force applied should not be so low that the tip gets retracted from the surface and also should not be too high that the tip indents the surface. An optimum force has to be applied by the

tip on the surface. This optimum force can be identified by obtaining "Force curves". Through force curves it is possible to measure the long range attractive or repulsive forces between the probe tip and the sample surface. The force curve is a means to understand local chemical and mechanical properties of surfaces like adhesion and elasticity.

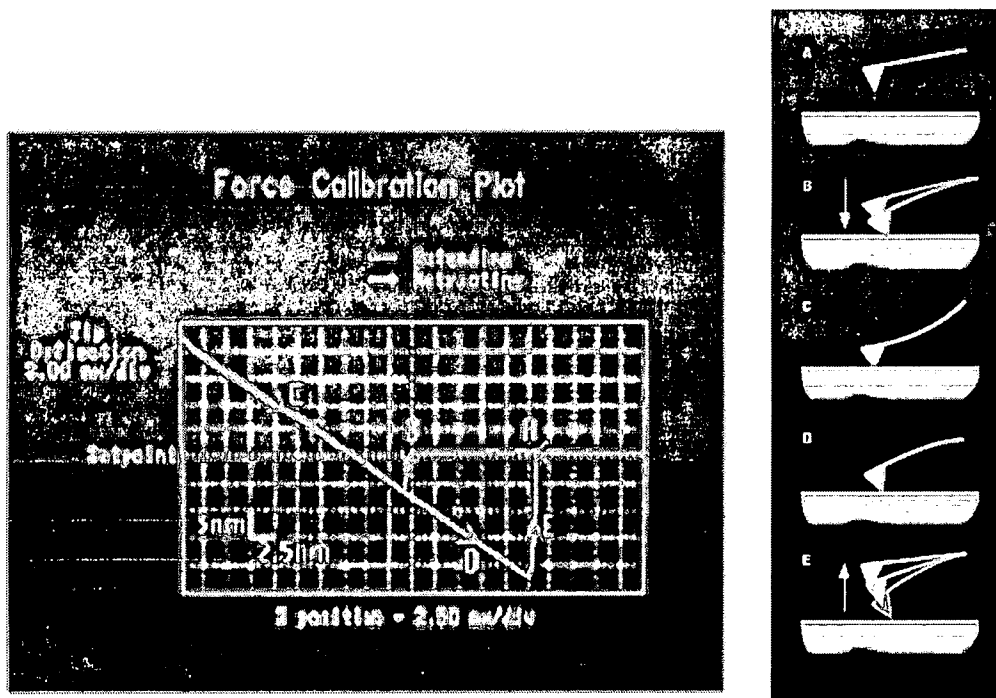


**Figure 14:** Typical force curve and the points along a force curve

A typical force curve of a Nanoscope III a system is shown in figure 14. Force curves typically show the deflection of the free end of the cantilever as the fixed end of the cantilever is brought vertically towards and then away from the sample surface. Experimentally, this is done by applying a triangle wave voltage pattern to the electrodes for the z-axis scanner. This causes the scanner to expand and then contract in the vertical direction, generating relative motion between the cantilever and sample. The deflection of the free end of the



cantilever is measured and plotted at many points as the z-axis scanner extends the cantilever towards the surface and then retracts it again. By controlling the amplitude and frequency of the triangle wave voltage pattern, the distance and the speed the AFM cantilever tip travels during the force measurement can be varied.

Some of the important features along a typical force curve are shown schematically in the figure. The beginnings of the cantilever's travel (A) not in contact with the surface. In this region if the cantilever feels a long-range attractive (or repulsive) force it will deflect downwards (or upwards) before making contact with the surface. As the tip is brought very close to the surface, it may jump into contact (B) if it feels sufficient attractive force from the sample. Once the tip is in contact with the surface, cantilever deflection will increase (C) as the fixed end of the cantilever is brought closer to the sample. If the cantilever is sufficiently stiff, the probe tip may indent into the surface at this point. In this case, the slope or shape of the contact part of the force curve (C) can provide information about the elasticity of the sample surface.

After loading the cantilever to a desired force value, the process is reversed. As the cantilever is withdrawn, adhesion or bonds formed during contact with the surface may cause the cantilever to adhere to the sample (D) some distance past the initial contact point on the approach curve (B). A key measurement of the AFM force curve is the point (E) at which the adhesion is broken and the cantilever comes free from the surface. This can be used to

measure the rupture force required to break the bond or strength of adhesive forces.

One of the first uses of force measurements was to improve the quality of the AFM images by monitoring and minimizing the attractive forces between the tip and surface. Large adhesive forces can reduce imaging resolution, damage the sample and probe and/or create unwanted artifacts. The force measurements in AFM are now increasingly used not only for improving the quality of images but also to investigate various types of forces between the surfaces, measuring the thickness of the adsorbed molecular layers, nano-indentation studies.

## **2.6) Tapping Mode AFM**

This mode (figure 15) overcomes problems associated with friction, adhesion, electrostatic forces, and other difficulties that plague conventional AFM.[19] The cantilever in tapping mode AFM is oscillated at the resonance frequency of the cantilever (50-500 KHz) using a piezoelectric crystal. The piezo motion causes the cantilever to oscillate with a high amplitude (typically greater than 20nm) when the tip is not in contact with the surface. The oscillating tip is then moved toward the surface until it begins to lightly touch, or tap the surface. During scanning, the vertically oscillating tip alternately contacts the surface and lifts off, generally at a frequency of 50,000 to 500,000 cycles per second. As the oscillating cantilever begins to intermittently contact the surface, the cantilever oscillation is necessarily reduced due to energy loss caused by the tip contacting

the surface. The resonant characteristics (like the amplitude and phase) are changed. The reduction in oscillation amplitude is used to identify and measure surface features. Silicon tips are used generally in tapping mode applications. The tip and the cantilever are an integrated assembly of single crystal silicon produced by etching techniques. These probes are much stiffer than the silicon nitride probes resulting in larger force constants and resonant frequencies.

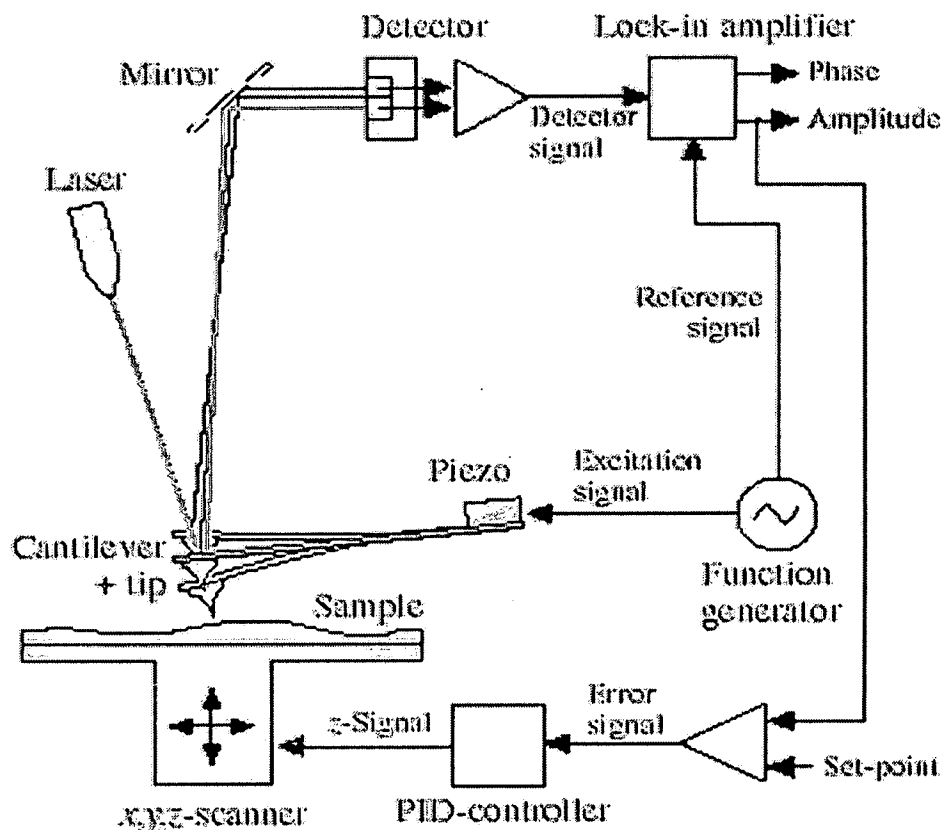


**Figure 15:** Schematic of tapping mode AFM

When the tip contacts the surface, the high frequency (50 - 500k Hz) makes the surfaces stiff (visco-elastic), and the tip-sample adhesion forces is greatly reduced. Tapping Mode inherently prevents the tip from sticking to the surface and causing damage during scanning. Unlike contact and non-contact

modes, when the tip contacts the surface, it has sufficient oscillation amplitude to overcome the tip-sample adhesion forces. Also, the surface material is not pulled sideways by shear forces since the applied force is always vertical. Another advantage of the Tapping Mode technique is its large, linear operating range. This makes the vertical feedback system highly stable, allowing routine reproducible sample measurements.

Apart from topographic measurements, phase and amplitude measurements can also be performed using Tapping Mode AFM. Phase measurement is used to detect the contrast in visco-elastic properties of the different materials across the surface. As the tip taps the sample surface, there will be a change in the amplitude and also a change in the phase angle of the cantilever compared with the free vibration amplitude and phase angle of the cantilever when the tip is not tapping the surface. This change in the amplitude and phase angle difference is measured by the feedback loop and the measurements can be made simultaneously with topographic measurements. The variations in the deflection amplitudes provide a measure of relative stiffness of the sample surface. The phase measurements in tapping mode can be related to the local elastic modulus in the image. Several researchers have utilized Tapping mode AFM to characterize the surface elasticity of materials.

In general, tapping mode AFM is one of the powerful tools for high resolution topography and surface elastic property measurements. Although it has several capabilities, the stiff cantilevers used lead to certain difficulties. It is very useful to characterize high hardness materials. On the other hand on soft

materials the changes in the elastic modulus is buried in the noise. In order to extract the elastic modulus information from these images several image enhancement and processing techniques have to be used. Generally cantilevers of different stiffness have to be used for different materials characterization.

## **2.7) Ultrasonic Force Microscopy (UFM)**

With the rapid advances in the field of manufacturing, it is now possible to make the micro devices' surfaces with little topography variations. Since AFM measures topographic data, there will not be much contrast in the images if the sample surface is almost flat. The images may provide little information on a scanning size of few microns and will appear to be blurred due to lack of topography. In order to have a better contrast and to be able to resolve nano scale features on the surfaces of micro-electronic devices, it is necessary to adapt AFM to measure surface elastic and other related properties on a nano scale. Studies were made to utilize tapping mode AFM to measure local elastic properties of the sample surfaces but the contrast was not so good partly because of the single resonant frequency and if the features happen to be less than the amplitude of the cantilever, those features cannot be resolved using tapping mode AFM. Ultrasonic force microscopy (figure 16) is an external modification to a conventional AFM operating with traditional contact tip-cantilevers. An ultrasonic transducer is attached to the one face of the sample. The opposite face is in contact with UFM tip. The piezo-electric transducer is

excited by a sinusoidal electrical signal in the frequency range of a few kHz to MHz. The acoustic waves propagating through thickness of the sample cause displacements in the z-direction. The amplitude of the displacement depends on the input amplitude of the electrical signal and the stiffness of the material under the tip. This displacement is measured using the AFM tip-cantilever. A schematic of the UFM used in this investigation is shown in figure. A function generator is used to excite the Piezo-electric transducer under the sample and the same signal is fed to one arm of a SRS Lock-in Amplifier.

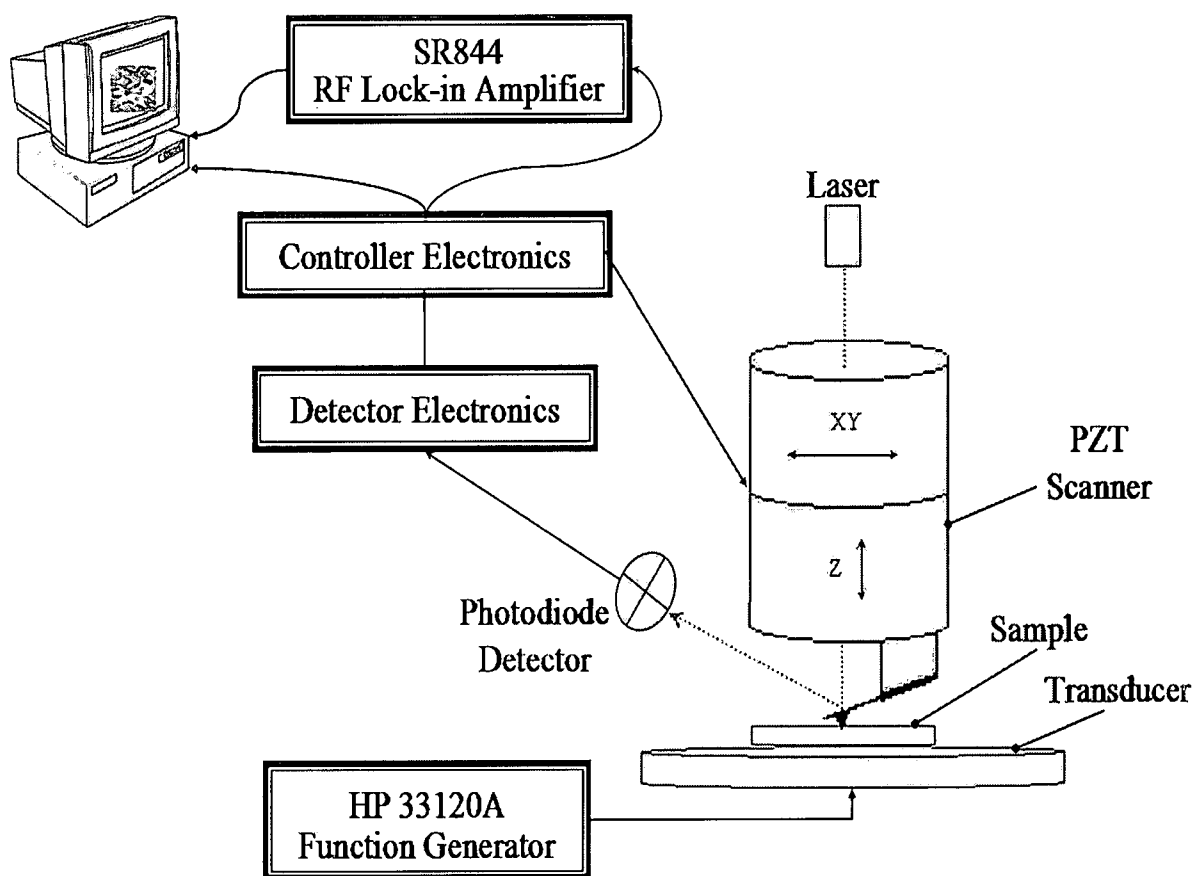


Figure 16: Schematic of UFM

The signal from the photo-detector that is proportional to the acoustic displacement is fed into the other arm of Lock-in amplifier. The differential amplitude or the differential phase is measured and the detector electronics is used to measure and display the UFM image. Most often the input amplitude to the piezo-electric transducer is kept low and UFM is operated frequencies not higher than first or second natural resonant frequency of the cantilever. These two conditions allow the tip to be in contact with the sample and hence the amplitude detected by the AFM tip can be directly related to the elastic modulus of the material under the tip [21-23]. This elasticity measurement can give clear information about defects, cracks, grain sizes and subsurface material changes in the sample surface beneath the tip. Higher frequencies have been used to perform UFM measurements but this requires nonlinear detection electronics and the image interpretation is more involved.

## **2.8) Contrast Due to Elasticity at Nano-scale**

The tip-sample interactions in AFM can be utilized to measure material properties. Several options are available to do these measurements. One of the techniques is force curve acquisition on the sample surface. In this method, force curve is measured at each point of the AFM image and it is analyzed to deduce the local elastic properties. Since force curves are obtained at each point in a scan, data acquisition times and data storage space is more in this technique. Another approach is to modulate the position of the sample at a frequency above

the highest system resonance and send the response signal to a lock-in amplifier to measure the signal's amplitude and phase [21]. The lock-in output is connected to the auxiliary data acquisition channels to form image. This method is called "Force Modulation" and an UFM system operates on this principle. The UFM used in this study utilizes a small amplitude continuous sine wave, to which the cantilever responds sinusoidally and stays in contact with the sample and is hence called contact mode.

The elastic contrast obtained in UFM images can be described by a simple explanation of contact mechanics. The tip-sample system in the AFM can be viewed as two systems in elastic contact and can be modeled by a Hertzian contact model shown in the figure 17.

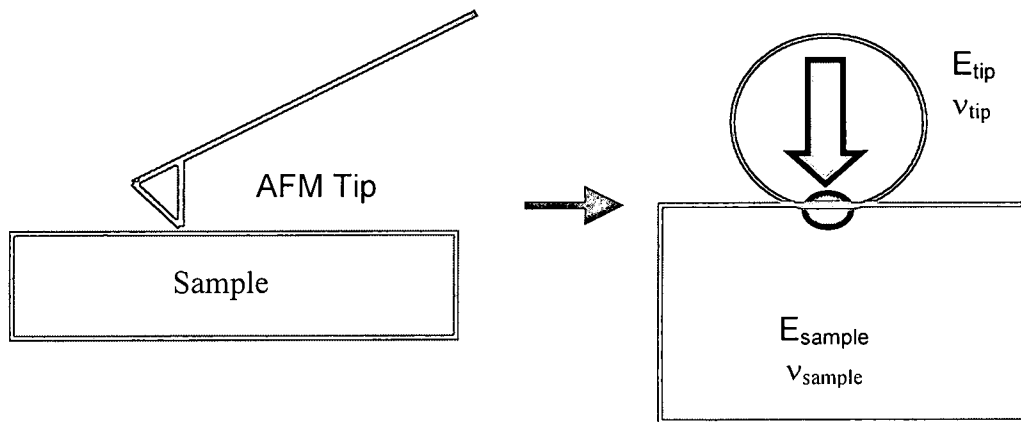


**Figure 17:** Tip –sample interaction modeled by Hertzian contact

The interaction stiffness ( $k_i$ ) of the sample and tip is defined as

$$k_i = \frac{3}{2} \frac{aK}{\dots\dots\dots} \quad (1)$$



Where  $K$  = reduced modulus of the tip and the sample and  $a$  = the contact radius between the tip and sample. The reduced elastic modulus of the tip and the sample is determined by Poisson ratio,  $\nu$  and Young's modulus,  $E$  and is given by the following equation:

$$\frac{1}{k} = \frac{3}{4} \left[ \left( \frac{1 - \nu_{tip}^2}{E_{tip}} \right) + \left( \frac{1 - \nu_{sample}^2}{E_{sample}} \right) \right] \dots\dots\dots (2)$$

The Young modulus of the tip and the Poisson ratio of tip and sample are assumed constant during the scanning. The only parameter that changes is the Elastic modulus of the sample. Thus the interaction stiffness changes in the image can be directly related to the changes in the stiffness of the sample. Thus the contrast seen in the UFM images is directly caused by the variations in the local elastic modulus of the sample surface. This explanation gives a simple qualitative model for the elasticity contrast in UFM images. A more elaborate model (figure 18) for UFM is developed by Burnham et al. This model relates the interaction of the tip of the AFM to the elastic variations of the sample surfaces under the AFM tip.

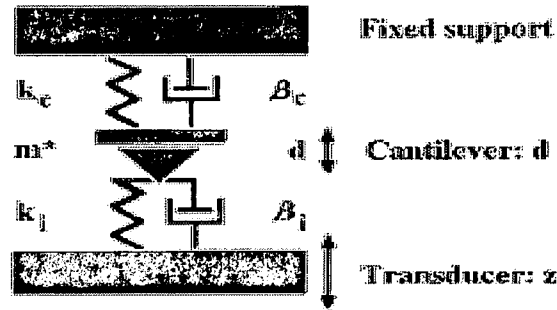


**Figure 18:** Rheological model for applying a displacement modulation to a transducer under a sample.

In this model, the base of the sample is modulated by a transducer and the tip position also changes sinusoidally. The cantilever is represented by spring stiffness  $k_c$ , damping constant,  $\beta_c$ , and effective mass,  $m^*$ . The tip-sample interaction stiffness is  $k_i(z, d)$  and its damping is  $\beta_i(z, d)$ , which are unknown parameters. If contact takes place at lower adhesive forces or high loads, tip-sample interaction can be written as

$$k_i(z, d) = 3Ka/2 \dots\dots\dots (3)$$

where  $a$  is the tip-sample contact radius and  $K$  is the reduced elastic modulus of the system. If the tip is stiffer than the sample, and the modulus of the tip and the radius of the contact area are known, the sample modulus can be obtained. The excitation amplitude in this model is assumed to be low so that the tip sample interaction stiffness and its damping are constant for a given load and the feedback circuit maintains a constant load. Two more assumptions have to be made in order to solve the above model analytically. Those are: 1) the interaction spring constant and interaction damping are constant for the small amplitude oscillation and 2) the interaction damping is low, i.e., the interaction is largely

elastic. The expressions for the positions of the transducer and cantilever and the equation of motion for the system are given by:

$$\begin{aligned} z &= z_0 + z_1 \cos \omega t, \\ d &= d_0 + d_1 \cos(\omega t - \delta), \\ m \ddot{d} + 2m \beta_c \dot{d} + k_c d &= 2m \beta (\dot{z} - \dot{d}) + k_i (z - d) \end{aligned} \quad \dots\dots\dots (4)$$

The subscripts 0 and 1 represent the dc and ac components of  $z$  and  $d$  respectively. The dynamic solution of the three equations given above gives expressions for the ac cantilever response amplitude divided by the ac transducer excitation amplitude  $d_1/z_1$

$$\frac{d_1}{z_1} = \frac{k_i [1 + (2m \omega \beta_i / k_i)^2]^{1/2}}{\sqrt{(k_i + k_c - m \omega^2)^2 + [2m \omega (\beta_i + \beta_c)]^2}} \quad \dots\dots\dots (5)$$

The above ratio is plotted as a function of frequency and as a function of  $k_i$  relative to  $k_c$  as shown in the figure 19.

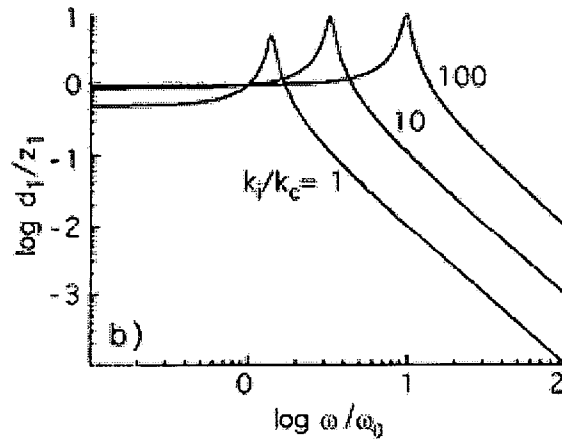


**Figure 19:** Plot of frequency Vs.  $d_1/z_1$

If a frequency is chosen within the region of the resonance, contrast inversion will occur, as parts of the lower-valued  $k_i/k_c$  are above some of the higher-valued  $k_i/k_c$  curves. Assuming low damping, the low-frequency limit is

$$\frac{d_1}{z_1} = \frac{k_i}{k_i + k_c} \dots\dots\dots (6)$$

which is the ratio of amplitudes expected from two springs in series. If  $k_c \ll k_i$ , the ratio  $d_1/z_1 = 1$  for all values of  $k_i$ . These are the typical operating conditions for the force modulation technique. For stiff samples a stiff cantilever or large amplitude modulation is used in force modulation, where either force sensitivity is compromised, or lateral sliding of the tip is induced by the large amplitudes, thereby degrading lateral resolution and incorporating frictional effects into the image.

The high frequency limit for  $d_1/z_1$  [23] is

$$d_1/z_1 = k_i/m^*\omega^2 \dots\dots\dots(7)$$

The ratio of the response to the excitation becomes linearly dependent on the interaction stiffness,  $k_i$  and independent of the cantilever stiffness. Thus weak cantilevers can be used to image elastic properties of stiff materials and maintain force sensitivity while measuring mechanical properties. UFM operates using soft cantilever at a frequency higher than the cantilever resonance, which eliminates dependence on the cantilever stiffness and thus allows for the better response for variations in the elasticity of the sample surfaces.

## 2.9) Experiment

The two objectives of this experiment were: i) to image the microstructure of the copper through a layer of polymer without having to remove the polymer and ii) to image the defects and changes in the microstructure of the copper while a constant current was passed through the sample. The sample used in this experiment was a flexible circuit sample which was described in detail in previous chapter. Nine flexible circuit samples from different manufacturers were imaged using the combination of AFM/UFM and tapping mode AFM to obtain microstructure of the copper buried underneath a layer of polymer. The sample was attached to a piezo-electric ultrasonic transducer using a tiny drop of honey to make the sample stick to the transducer. Honey acts as a coupling medium through which the ultrasonic waves propagate through the sample. The input signal to the transducer was given by a function generator (HP Model # 33120 A) which generated a low amplitude sinusoidal wave in the range of 100 KHz- 1 MHz. Simultaneous acquisition of both AFM and UFM images was made possible by using the electronic feedback signal from the AFM's topography image and inputting the signal through a filter and separating electronic loop. This loop was used to separate the ultrasonic image (high frequency) from the topography image (low frequency). A lock-in amplifier (Stanford Research Systems Model # SR844RF) detected the amplitude and the phase change of the ultrasonic response signal relative to the input signal from the function generator. This change in the amplitude or phase was then sent to the computer

through a feedback loop and recording the ultrasonic force image of the sample surface.

The flex circuit sample was carefully attached to the ultrasonic transducer using a tiny drop of honey. First, the AFM tip was engaged with the sample surface and a good force curve was acquired. After a good force curve was obtained, the sample was scanned and a topographic image obtained. Once a good topographic image is acquired, the ultrasonic image is obtained by selecting an optimized frequency range. This is done by varying the amplitude and the frequency of the input signal and monitoring the output signal of lock-in amplifier for maximum signal. The frequency at which there is a stable maximum signal is selected for imaging. The maximum signals were observed at four to five different points in the range of 100 KHz- 1 MHz. The feedback controls like set point, gains, were adjusted suitably to obtain good contrast topography and ultrasonic images simultaneously.

The second part of the sample required a current to be passed through the sample while scanning the sample using AFM-UFM. Current was passed through one of the samples which was micro bonded for the purpose. A DC power source was used to send in a current through the flex circuit. Images were taken in-situ while the current was passed through the sample.

## **CHAPTER 3**

### **MICROSTRUCTURAL ANALYSIS**

#### **3.1) Importance of Microstructure**

Microstructure of a material gives information about the grains, particle sizes, dislocation densities, micro-cracking etc. Properties like yield strength, elastic modulus and many other properties of the engineering materials are directly related to the microstructure of the material. The processing conditions of a material decide its microstructure. Since the microstructure of the material determines the properties of the material, the study of the microstructure can reveal a direct causal relationship between a particular microstructural feature and a specific property. As the size of the electronic devices gets smaller, study of microstructure becomes important for the reliability studies. Microstructure of a material also gives information about defects, voids, and unwanted inclusions in the material. A defect or crack even on a nano scale can cause failures in the micro-electronic devices. Nano-sized defects present in the metal, polymer or interface of the copper/metal of a flex circuit can be known by the study of the microstructure. Thus it is important to study the microstructure in order to assess the reliability of the product. Apart from information about defects, microstructure of the copper is used as a quality control factor in hard disk drive industry.

Flex circuits with a favorable copper grain size and orientation has to be used on the arm of the hard disk drive for maximum life of the product. This information along with the defect analysis may be utilized to study the reliability of the flex circuits in the head slider assembly of the hard disk. Conventional techniques like TEM, EBSD have been used to study the microstructure of copper previously. But these methods cannot be used because of the presence of a polymer layer on the copper film and moreover these methods require extensive sample preparation. High energy X-rays have been used to study microstructure through a passivation layer but its relative lack of resolution limits its usage for the present problem. A hard disk manufacturer acquires flex circuits from different vendors and if a quality control study has to be performed by way of studying the microstructure, the polymer layer on the top of the copper layer has to be removed and then the microstructure imaged. This can be time consuming and expensive. In this study, AFM/UFM has been used to image the microstructure of the copper without removing the layer of the polymer layer on it.

### **3.2) Advantages of AFM-UFM in Microstructural Analysis**

The technique of AFM-UFM has been used previously to study the individual grains of copper without any extensive sample preparation or chemical etching [24]. Conventional methods to image the microstructure require sample preparation and chemical etching of the surface to be imaged. Apart from the chemical etching of the surface, the polymer layer on the copper film in a flex



circuit has to be removed in order to obtain the microstructure. AFM has been used to image the microstructure of the copper microwires with minimal sample preparation and it provides a quicker and easier way for device and quality control analysis for micro electronic devices. UFM senses the signal coming through the sample and detects the changes in the local elasticity changes on the sample surface thus facilitating imaging of the microstructure of copper under a polymer layer. This technique will allow non-destructive evaluation of the microstructure after the device has been in use thus making it a valuable tool to study the changes in the microstructural changes in the devices.

### **3.3) Flex Circuit Samples Studied**

Nine different flex-on suspension (FOS) flex circuits from different vendors were imaged in this experiment. Fig shows a schematic of a FOS flex circuit along with its components. To read/write data from/to on to the hard disk, signals have to be transmitted between the pre-amplifier of the flex circuit and the GMR head slider assembly. The GMR head slider assembly is soldered onto the other end of the flex circuit. The two signals that are transmitted between the pre-amplifier and the head slider assembly are called Read Signal and Write signal. The signals are passed through copper wires (approximately 200  $\mu\text{m}$  wide) which are shown in figure 20. The head slider assembly is soldered into the holes drilled near the copper lines of the flex circuit. The read/ write signal copper lines on the flex circuit were selected for imaging of the microstructure of the copper

because head slider assembly is soldered in to the holes and hence it is important to study any changes in the microstructure of copper at this region in different flex circuits. Apart from imaging at the above mentioned region, some more regions were also selected for imaging to see any variations in microstructure of the copper.

### **3.4) AFM-UFM Results**

This section gives an overview of the results of the microstructural analysis obtained on different flex circuits. The flex circuit samples are numbered from 1 through 8. On each of the sample, AFM-UFM was used to image the microstructure at different places with the most emphasis on the region where the head slider assembly is soldered. Tapping mode was also used on some of the samples to compare the contrast from that of UFM images. Figure 21 shows an AFM-UFM image obtained on sample # 1. An optical image showing the region of imaging on the flex circuit is also shown in figure 20. All the images were obtained on all the flex circuit samples in the regions similar to that shown in this figure. The image was taken with a scan size of 3 microns with an ultrasonic frequency of 550 KHz. The height scale in this image was 0-800 nm with some features more than 800 nm at some places. Those areas are seen as bright areas in the image.

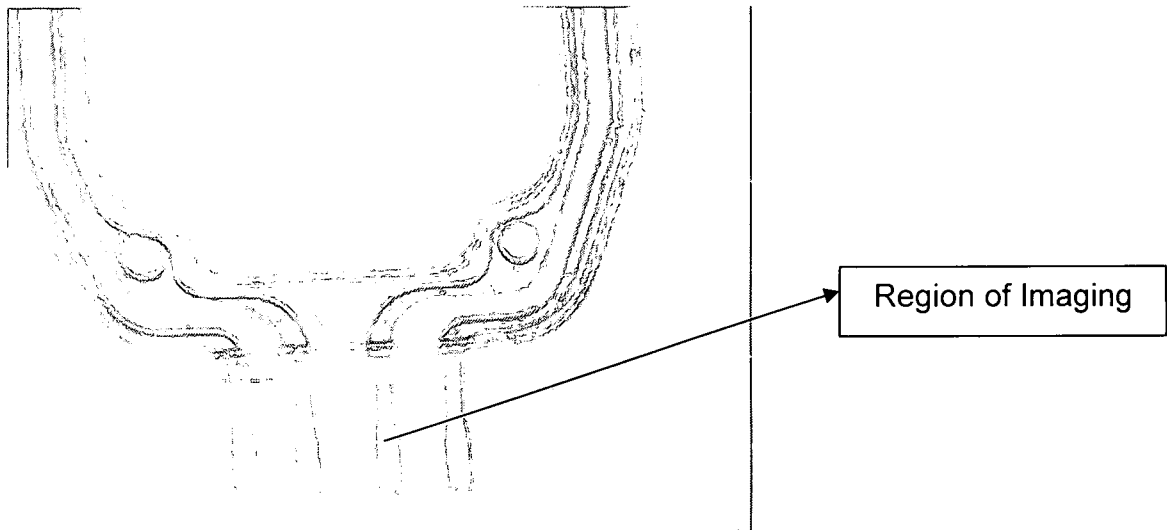


**Figure 20:** An Optical image of the flex circuit

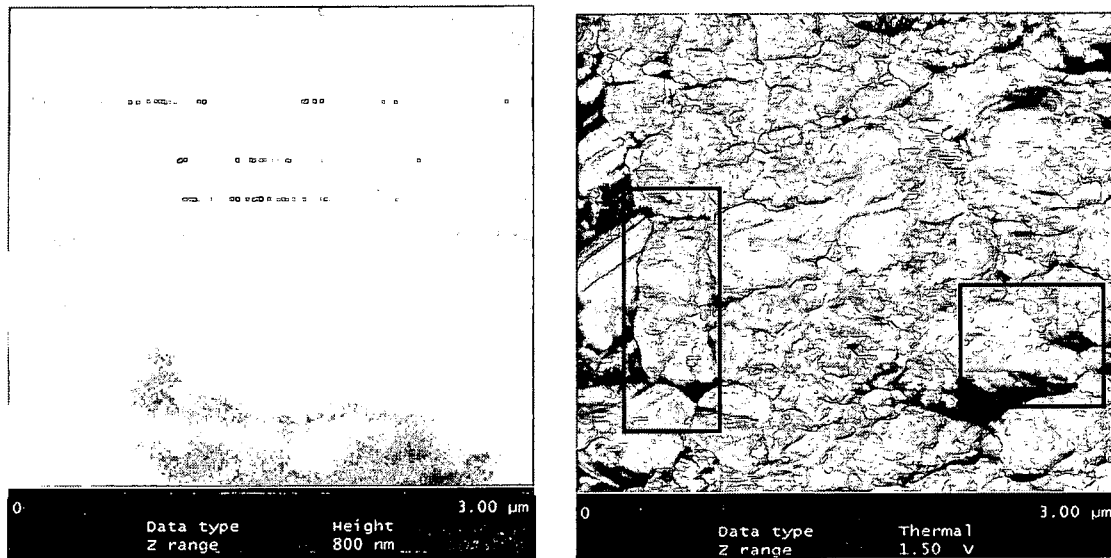


**Figure 21:** AFM-UFM image of copper on sample #1

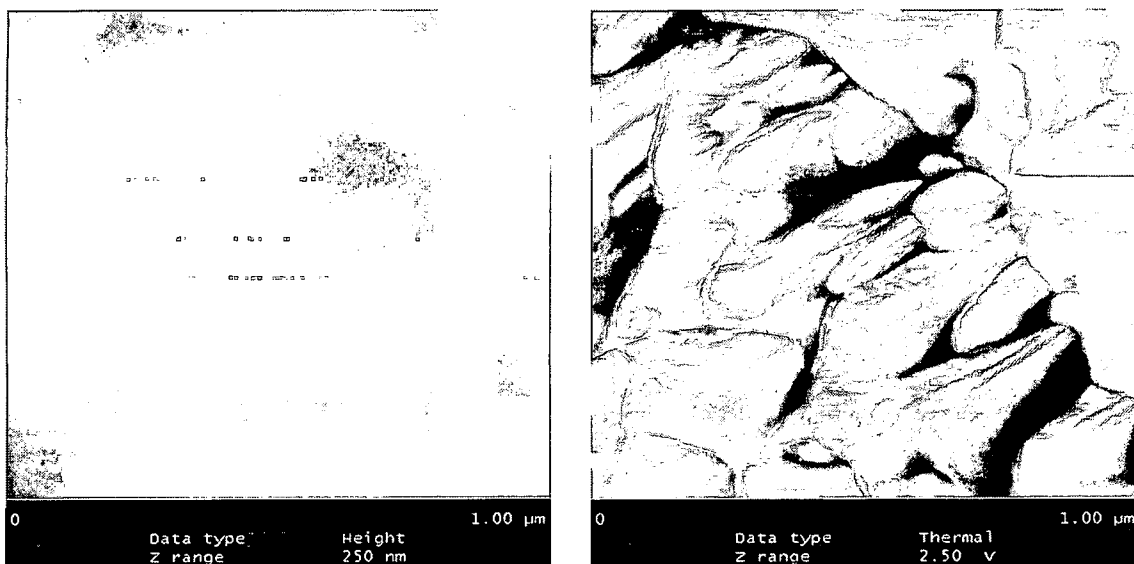


**Figure 22:** AFM-UFM image of the same region with different frequency and scan size

The microstructure of the copper through the polymer layer can be clearly seen in these images. While the left image shows an AFM image which is essentially a topography image, the right image is an UFM image showing the local elasticity information of the sample surface. The difference in the contrast from AFM and UFM image can be very clearly seen in the images. The AFM topography image shows some details about the microstructure of the copper but the UFM image shows individual grains and grain boundaries with clear. The images were taken at two different places on the same copper line (Fig 20). Figure 22 is a smaller scan area image of the copper line at a different region at the same frequency which shows the clarity of the grains in the UFM image. The region inside the box in figure 21 shows nano sized particles which may be either voids or air trapped in between the layers of copper and polymer. These particles are seen in UFM image. The image also shows a marked change in the contrast in the grains on the left side of the image and right side of the image. The darker

regions of the grains are those grains which have higher stiffness than other grains. The region is shown by a box in the image. Another image was obtained on the same copper line but at a different region and the image shows microstructure with grain size slightly greater than the grain size at the previous region. To obtain a quantitative value for the grain size of the copper from an AFM image can sometimes be very difficult. Even with the help of image enhancement techniques, the AFM topography information will give little information about the grain size. But the UFM image of the same region shows the details of an individual grain and grain boundaries with clear contrast facilitating easier discerning of the grains. The enhanced contrast is due to elastic anisotropy of the copper in the flex circuit. The grain sizes of the copper were calculated using the UFM image. The individual grains in the image were counted and dividing the total number of counted grains by the area of the region of the imaging and assuming a circular structure to the grains. The average grain size of the copper in this sample using this method was approximately around 450 nm.

Figures 23 and 24 show the microstructure of the copper of sample # 2 flex circuit obtained at two regions along a read/write signal copper wire. The UFM image shows a similar contrast to that of obtained on sample # 1. The grain size of the copper in this sample was smaller than the previous sample. Grain size variations in copper can be observed in this sample with the grain sizes ranging from 100 nm to 550 nm. These images were taken on a scan size of

2 $\mu$ m and 3  $\mu$ m with a frequency of 475 KHz. The topographic data scale in this sample was 0-400 nm which was half that of the previous sample.

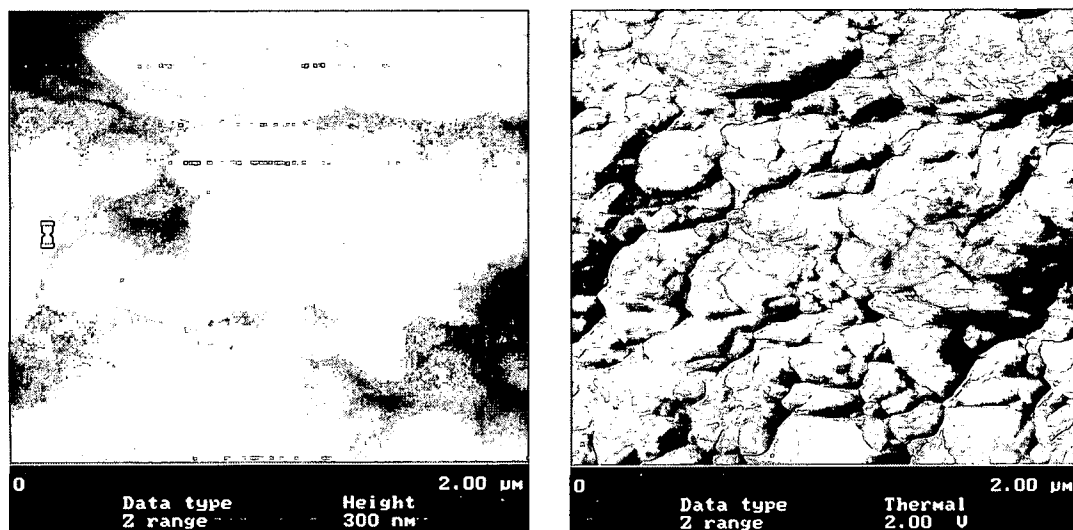


**Figure 23:** Microstructure of copper on sample # 2

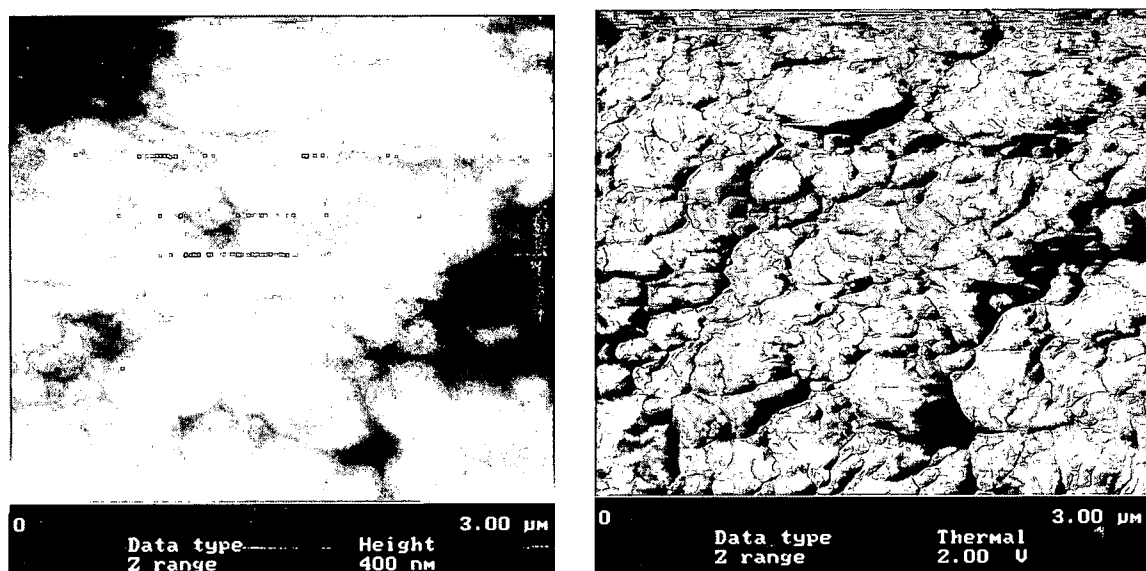


**Figure 24:** Microstructure of copper on Sample # 2 at a different location on the same copper line

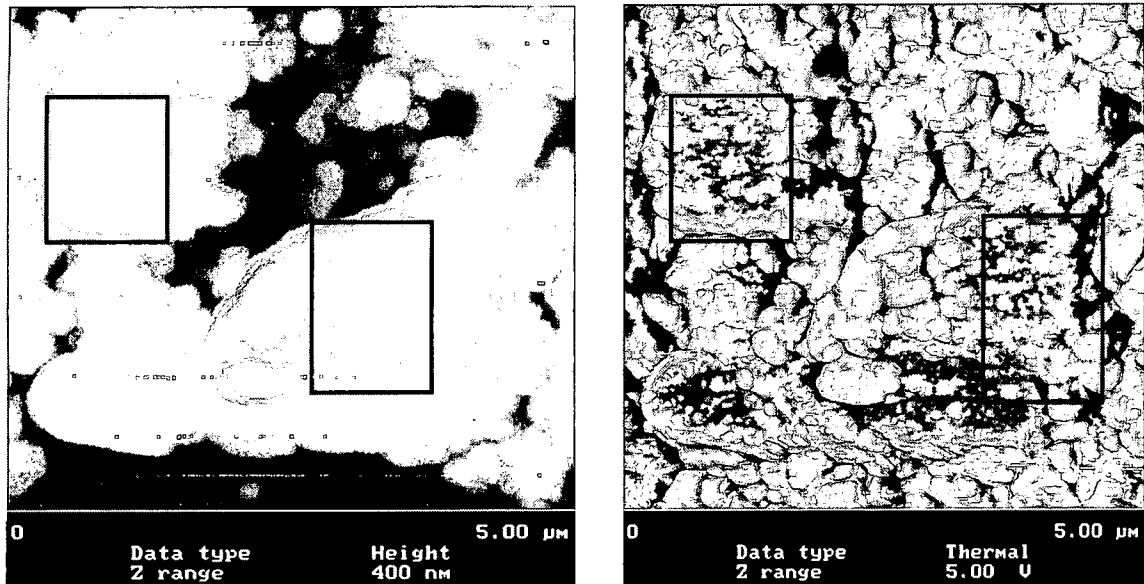


**Figure 25:** Microstructure of copper in sample # 3

The above figure shows the microstructure of the copper of flex circuit sample # 3 in the region similar to the region shown in figure 20. Apart from the grains and grain boundaries, this image also shows nano sized particles (approximately 80nm) in the region shown in the box. These particles may be defects in the polymer or air trapped in between the layers of polymer and copper. These particles are clearly seen in the UFM image with better contrast. The grains of copper in this sample are smaller and more spherical than the other previous flex circuit samples.

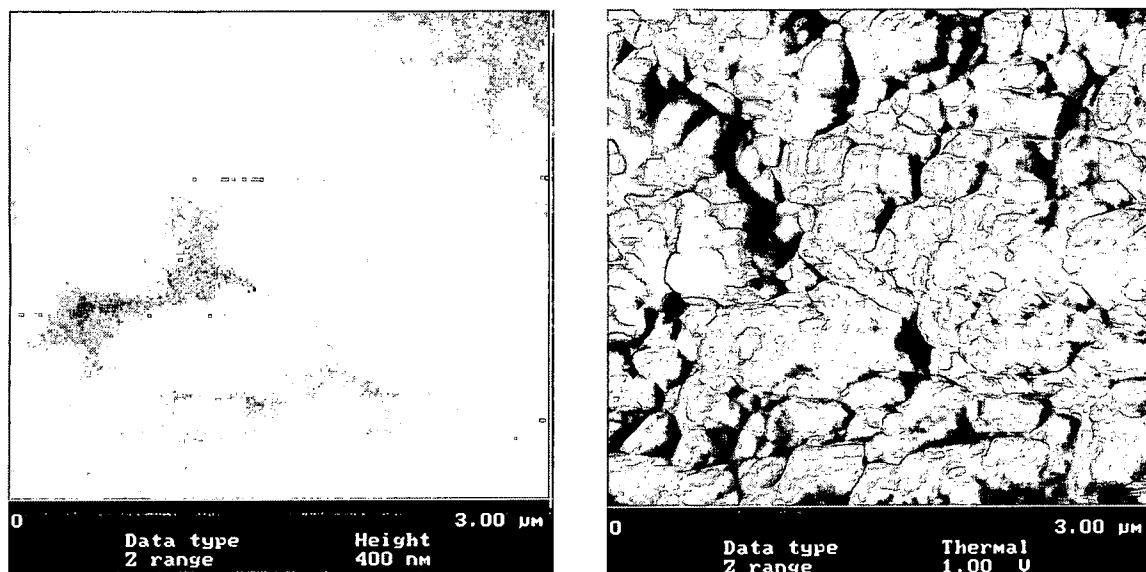


**Figure 26:** Microstructure of copper on sample # 3 obtained at a different region

The figure above shows the microstructure of the copper on sample # 3 at a different area on the same copper line. This image does not show any defects or voids as the previous image and the grain sizes and shape of the copper is similar to the size and shape of the copper obtained at the previous region with the average grain size of the copper at 350 nm.

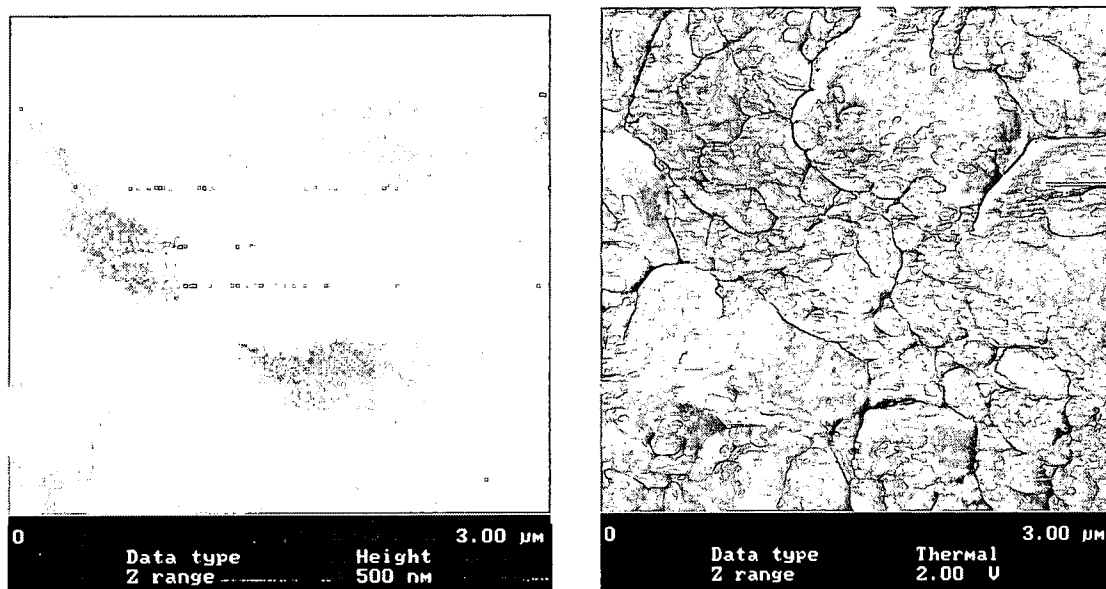


**Figure 27:** Microstructure of copper in sample # 4



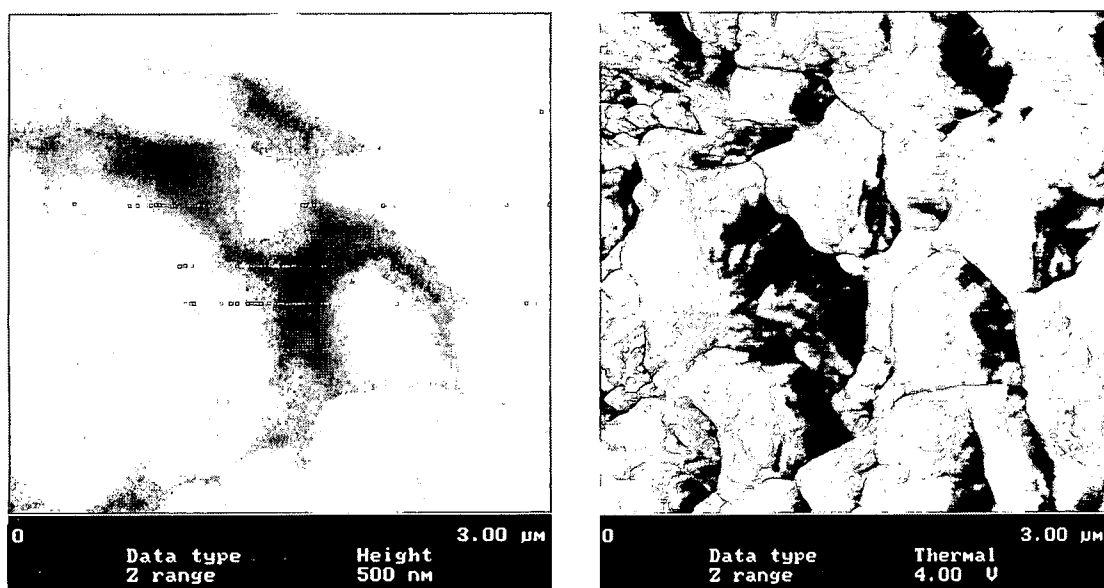
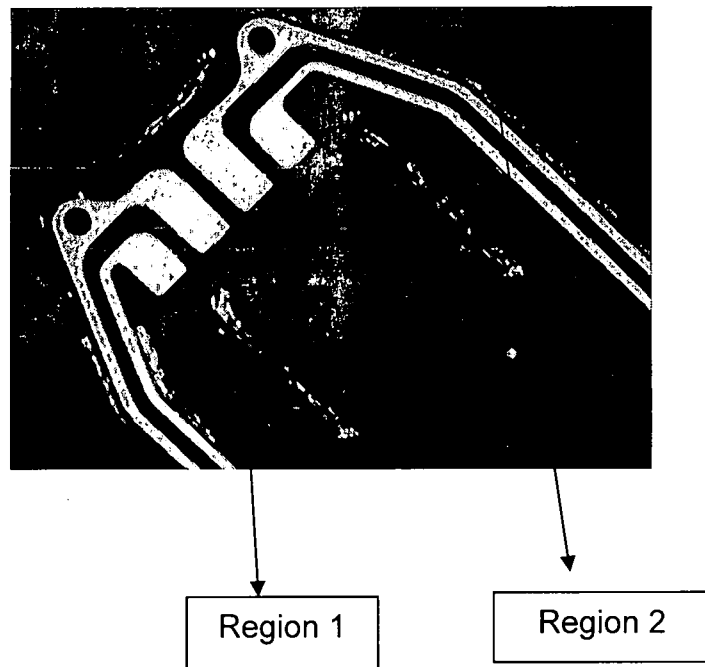


**Figure 28:** Microstructure of copper of sample # 4 at a different region on the copper line.

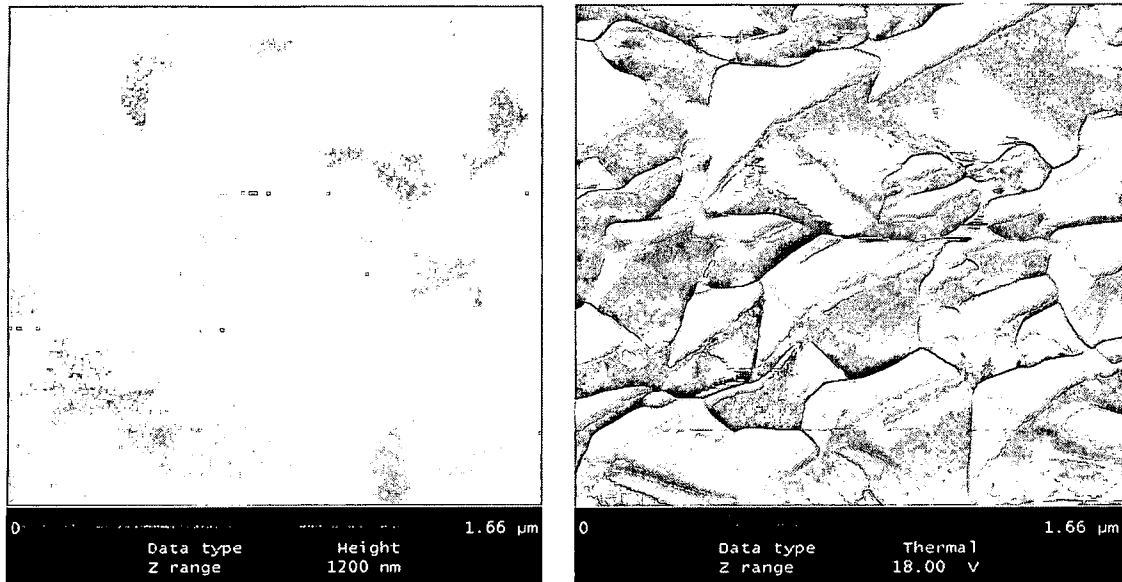
Figures 27 and 28 shows the microstructure of the copper on sample # 4 with a scan size of 3  $\mu\text{m}$  at two different regions on the same copper line. These images show variation in the microstructure at two different regions of the flex circuit. Figure 27 shows the variation in the size of the copper grains and the contrast in grains. The size of the copper grain was ranging from 200 nm to 500 nm. The microstructure at a different area on the copper line (figure 28) shows a marked difference in the size and the shape of the copper grains from the previous region. The size of the grains at this area is much bigger than the size at the first region and also, while grains in the first region were mostly spherical in first region, they were pyramidal in the second region.

Figure 30 shows the microstructure of the copper on another flex circuit sample. The image was taken on the region 1 of the flex circuit (figure 29) with a scan size of 1.66  $\mu\text{m}$  and an ultrasonic frequency of 125 KHz. Figure 31 shows the microstructure of copper taken in region 2 of the sample with a scan size of

2.08  $\mu\text{m}$  and a frequency of 125 KHz. The microstructure did not show any changes in the two regions but the average grain size of the copper in region 2 (750 nm) was slightly greater than the average grain size of the copper in region 1 (600 nm). The topographic data scale for these images was 0-1200 nm which was higher than other flex circuit samples. The clear contrast obtained in the UFM images is due to the anisotropic property of copper and in this sample, the grains are oriented in different directions, thus showing the grains and grain boundaries with good contrast.



**Figure 29:** Optical image of the flex circuit sample # 5



**Figure 30:** Microstructure of copper on sample # 5 on region 1

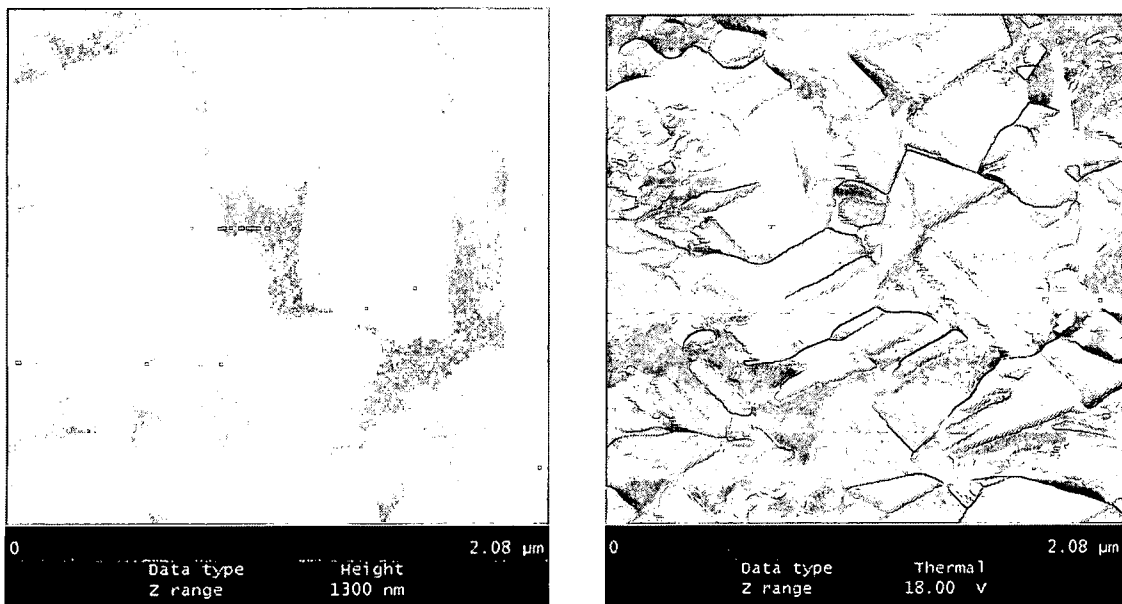


**Figure 31:** Image obtained at region 2 of sample # 5

AFM-UFM images (figures 32 and 33) of the next sample showed no microstructure of the copper and it was dominated by defects in polymer or at the interface of copper and polymer. Two regions, similar to the regions of the previous sample, were selected on this sample and both regions showed lot of defects in the polymer. The average size of the defects was around 80 nm. The

presence of these defects may be either due to the processing defects during the manufacturing of the flex circuits, or due to the presence of defects in the raw material of the polymer.

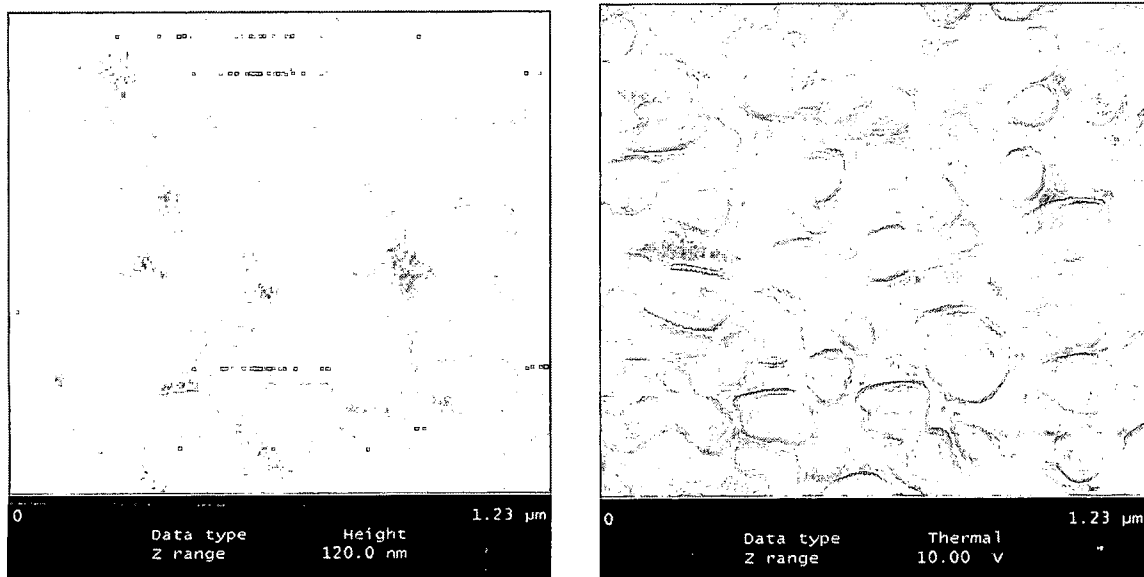


**Figure 32:** Image obtained at region 1 of the sample# 6

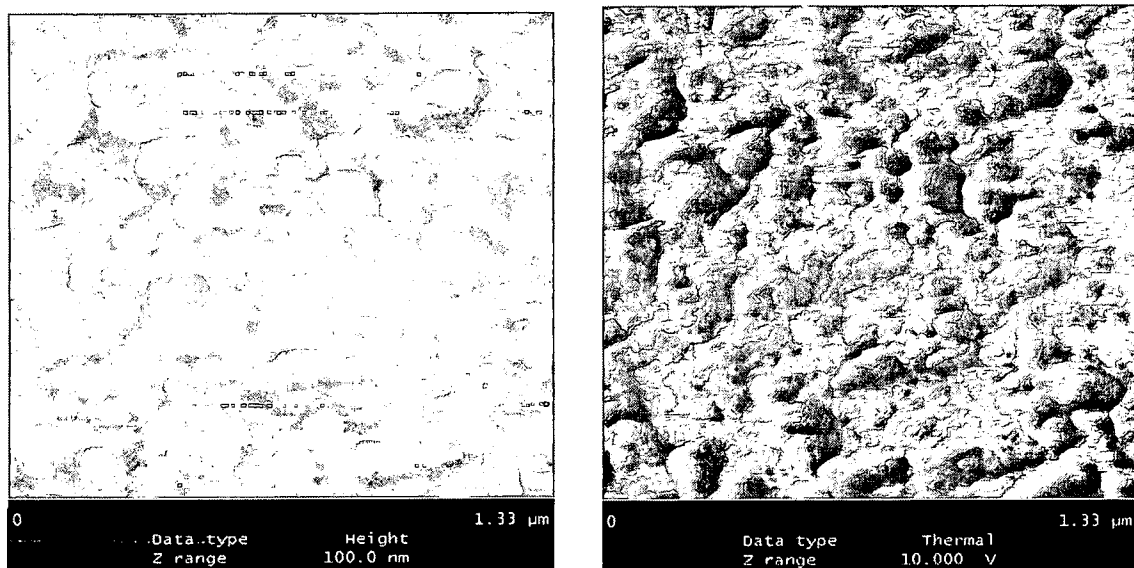


**Figure 33:** Image obtained on region 2 of sample # 6

The next sample imaged showed a uniform microstructure (figure 34) along the read/write copper lines of the flex circuits. Along with the uniform microstructure, nano-sized particles are seen in the UFM image with an average size of 30 nm. Some of these particles are shown by arrows in the figure. The presence of these nano sized particles may be due to air trapped in between the layers of polymer and copper during the lamination of polymer and copper films. The uniform microstructure may be due to the uniform crystallographic orientation of the grains and thus no contrast can be seen from grain to grain. The average grain size in this region was 380 nm.

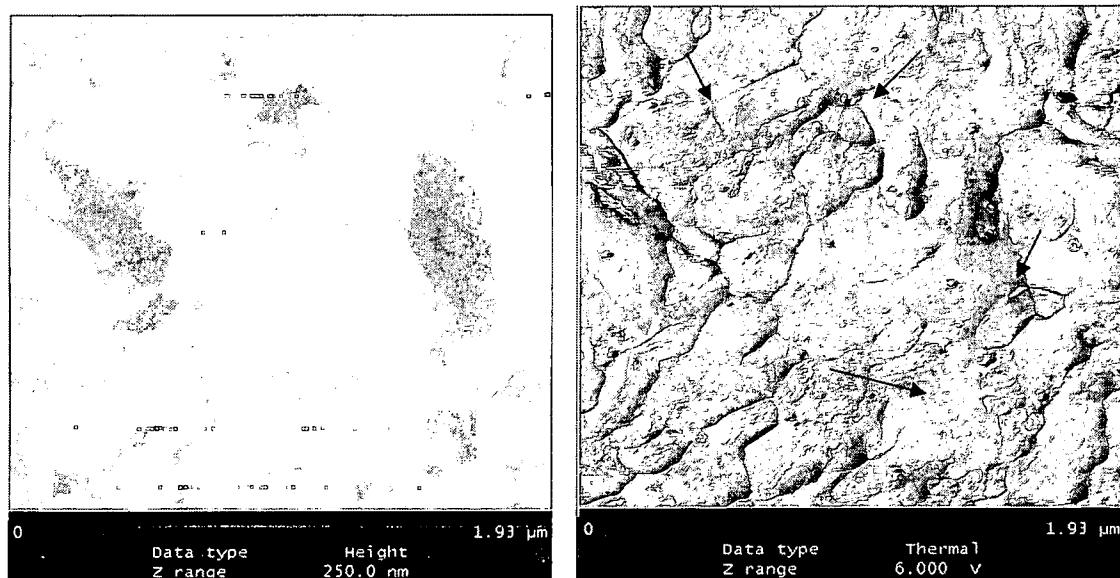


**Figure 34:** Uniform microstructure of copper in sample # 7 (region 1)

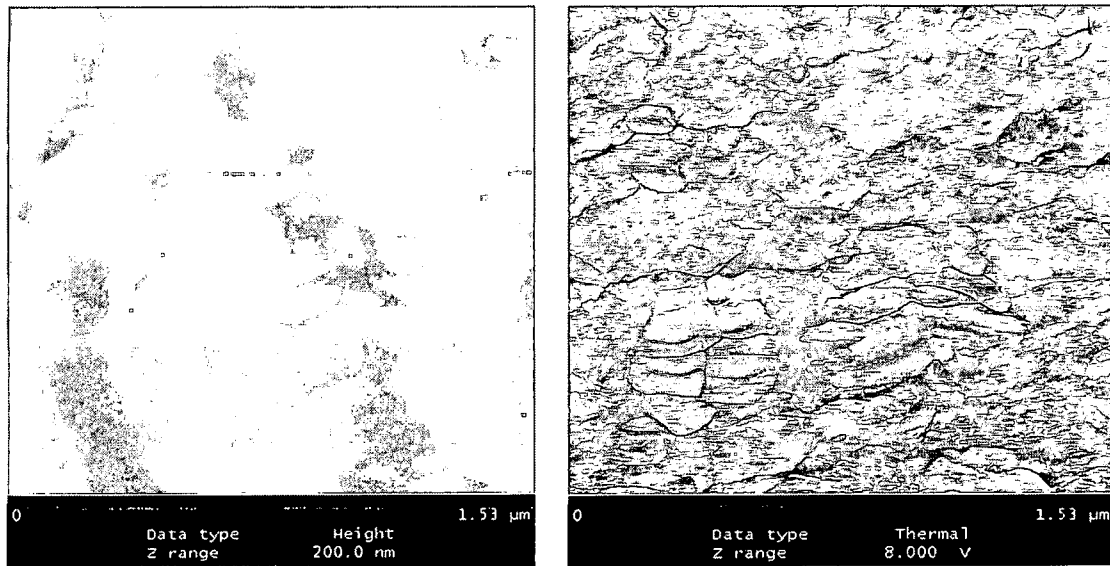
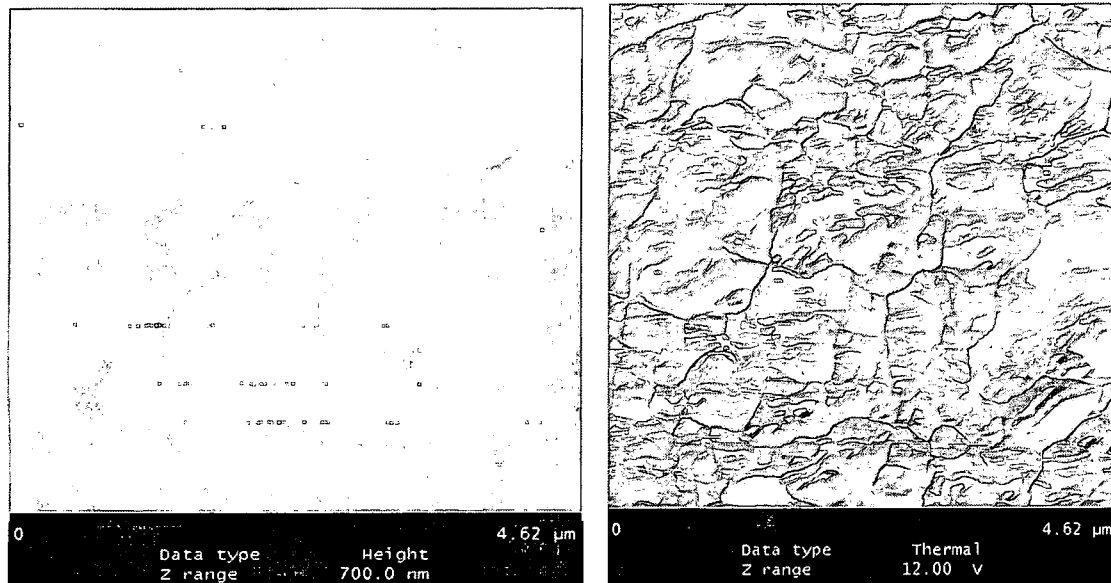


**Figure 35:** Microstructure of copper at region 2 of sample # 7

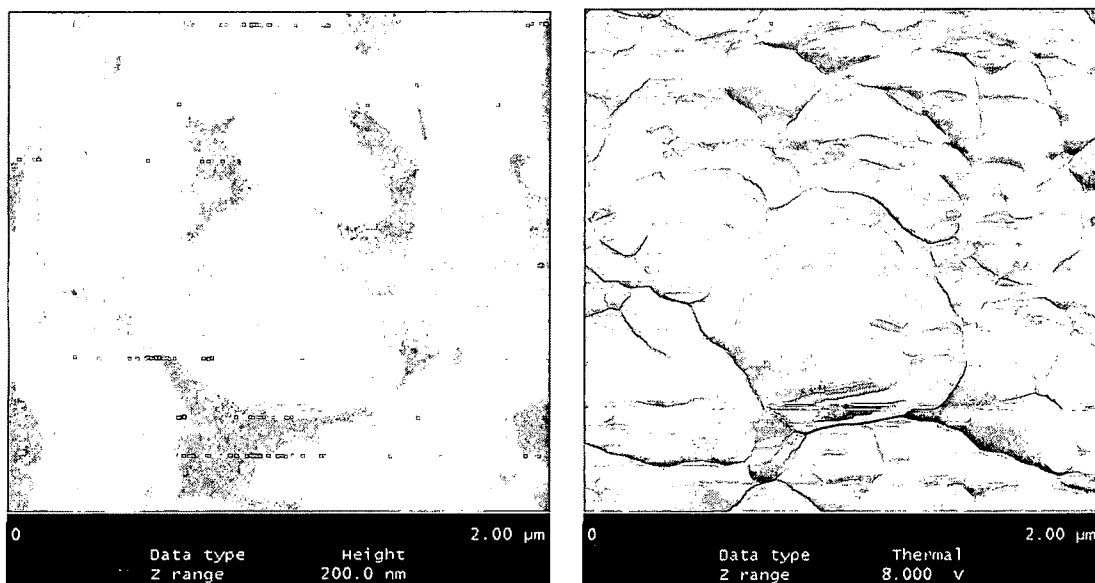
Image taken on the region 2 of the sample showed a slightly non-uniform microstructure (figure 35) of copper at some regions with some grains showing contrast at some areas and with no contrast at most of the areas of the image. Also, the grains appear to be elongated in one direction in this image which has an average grain size of around 400 nm. The image also shows some nano-sized defects at some regions.

Figure 36 shows an AFM-UFM image of the region 1 on flex circuit sample # 8. The image shows larger grain sizes and also formation of twin grains inside a grain. The formation of these twin grains can be attributed to the processing conditions of the copper. The average grain size of the copper in this region was 700 nm. Clear contrast can be seen from grain to grain in this image because of different crystallographic orientation of each copper grain. Imaging on the region 2 of the sample (figure 37) revealed larger grains than the previous region. The average grain size in this region was 750 nm. The formation of the twin grains

was not observed in this region of the sample. The microstructure also was relatively uniform because of uniform orientation of the grains in this region.



**Figure 36: Microstructure of copper on sample # 8 (region 1)**



**Figure 37: Microstructure of copper on sample # 8 (region 2)**

The samples imaged so far, have not shown much variation in microstructure from region 1 to region 2. Figure 38 and 39 shows AFM-UFM images obtained on sample # 9 which shows drastic variation in the microstructure of the copper at the two selected regions for imaging. The microstructure at region 1 shows a uniform microstructure of copper with the average grain size around 370 nm and with a pyramidal shape of grains. The microstructure in region 2 shows a non-uniform structure of copper along with defects in the polymer. The grain size of the copper in this region is approximately half the grain size of the copper at region 1. The shape of the grains also showed a variation with the grains mostly spherical in this region as compared to the pyramidal shape in region 1.

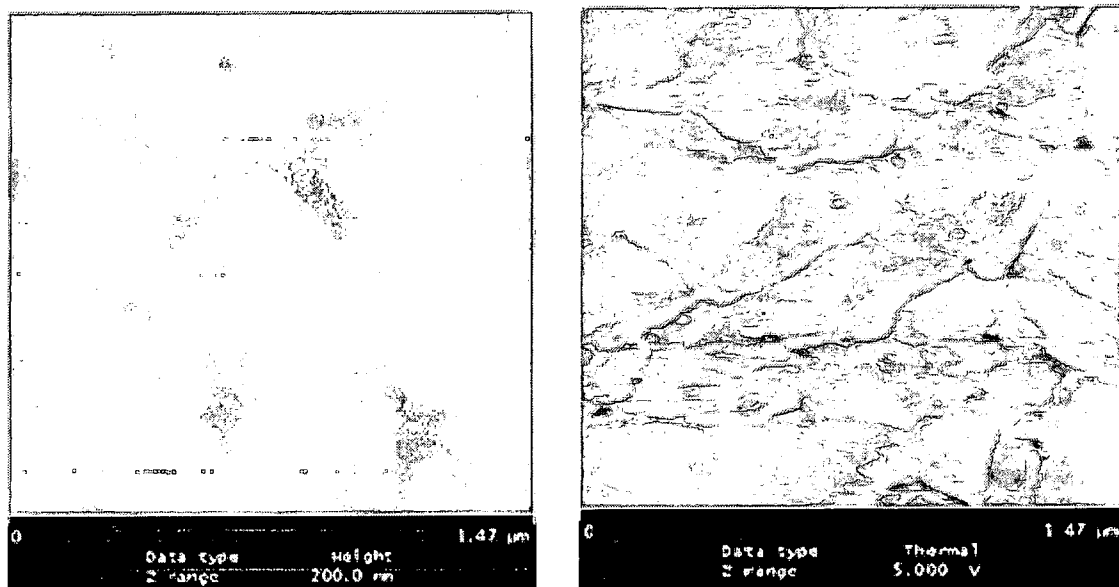


**Figure 38:** Uniform microstructure of copper in region 1 of sample # 9



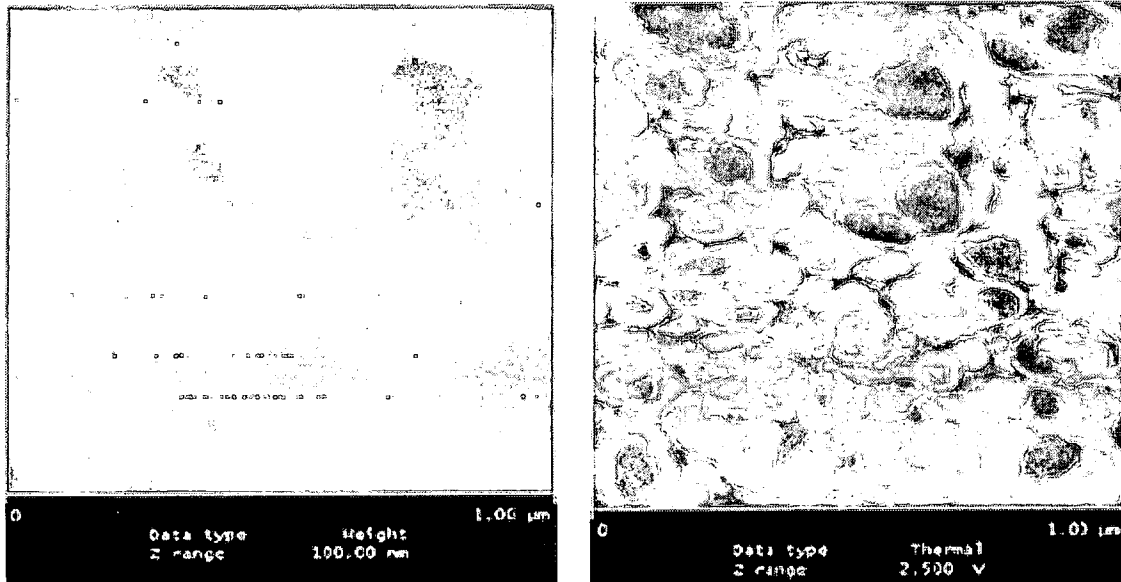


**Figure 39:** Microstructure of copper at region 2 of sample # 9

### 3.5) Tapping Mode AFM Results

Tapping mode AFM was also used on one of the flex circuit samples. In tapping mode AFM, a silicon tip is vibrated at a frequency of 200-400 KHz, slightly tapping the sample surface during the vibration cycle. There will be no lateral forces acting on the sample surface in tapping mode AFM thereby decreasing damage to samples. As the tip taps the sample surface, there will be a change in the amplitude and also a change in the phase angle of the cantilever compared with the free vibration amplitude and phase angle of the cantilever when the tip is not tapping the surface. This change in the amplitude and phase angle difference is measured by the feedback loop and the measurements can be made simultaneously with topographic measurements. The variations in the deflection amplitudes provide a measure of relative stiffness of the sample

surface. The phase measurements in tapping mode can be related to the local elastic modulus in the image. UFM is used to detect local elasticity changes in the sample surface when an ultrasonic wave is sent through the sample. So tapping mode AFM's amplitude or phase image and an UFM image gives similar information about the elasticity of the sample surface. This section discusses the results obtained by using tapping mode AFM on one of the flex circuit sample and compares those images with images obtained by the combination of AFM-UFM.

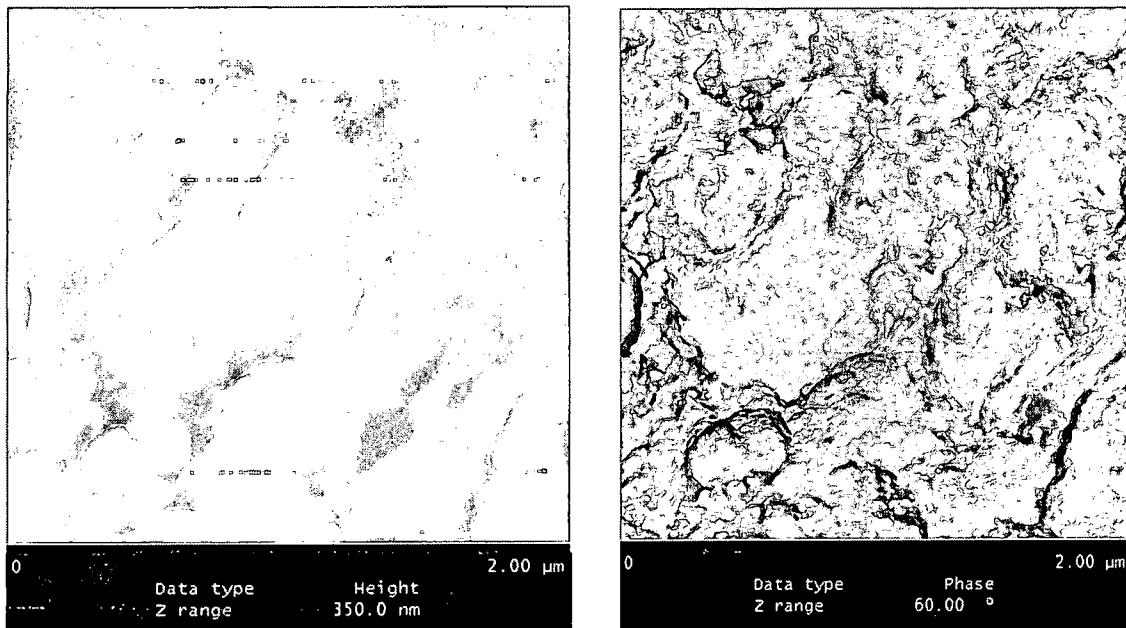


**Figure 40:** Tapping mode AFM image of copper on a flex circuit.

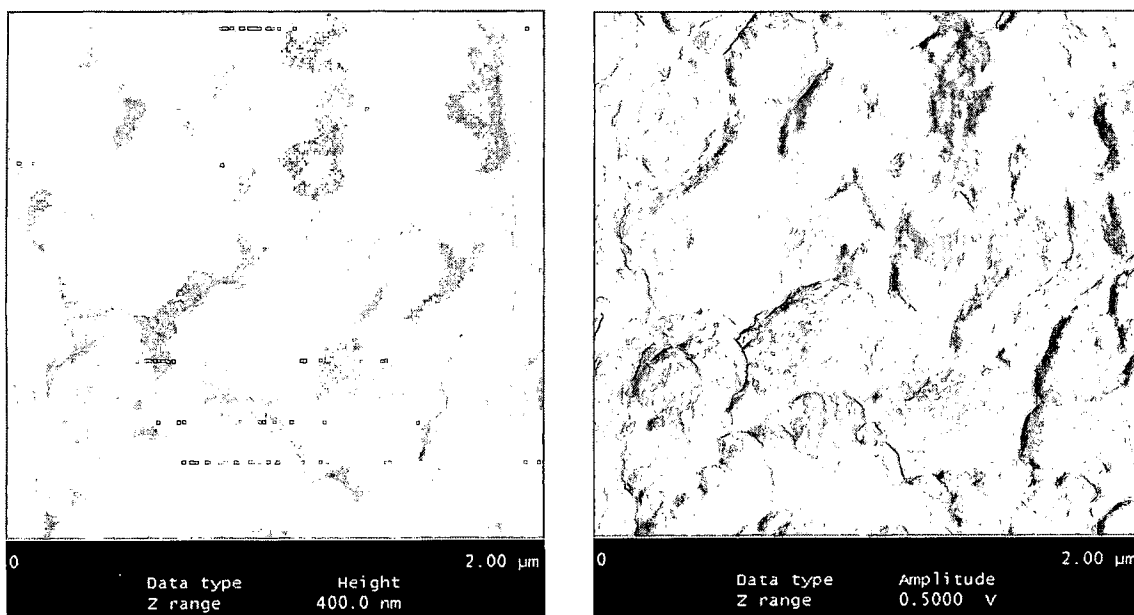


**Figure 41:** Topographic and amplitude images (Tapping Mode AFM) of copper on flex circuit.

Figure 40 shows topography and phase image on the flex circuit sample. The phase image gives information about the relative stiffness of the sample surface by recording the changes in the phase of the oscillation of the tip when it touches the sample surface. The contrast in this image is similar to that of an UFM image but nano scale features cannot be resolved very clearly using tapping mode AFM. The reason for this lack of better contrast when compared to an UFM image is that UFM employs different frequencies in the range of 300 KHz -1 MHz and a higher frequency ultrasonic wave can result in a better contrast image, while tapping mode has a single frequency of vibration and this frequency may not be sufficient to resolve some of the nano particles with better contrast. Figure 41 shows topography and amplitude images of the same region using tapping mode. Amplitude image of tapping mode measures the relative changes in the amplitude of the cantilever when the tip contacts the surface and

the image is a measure of the relative stiffness of the sample surface. The amplitude image of the tapping mode does not show much contrast when compared to the amplitude image of UFM. The reason is again due to the single frequency of the vibration of the cantilever which may not be sufficient to resolve the grains with better contrast.

### **3.6) Discussion of the Microstructure Analysis Results**

The combined technique of AFM and UFM was successfully implemented to image the microstructure of the copper through a layer of polymer, approximately 7  $\mu\text{m}$  thick. Apart from the microstructure of copper, nano-sized defects present in the polymer layer were also imaged in some of the samples. The non-destructive evaluation of the copper microstructure without removing the layer of polymer in a short time makes this technique a valuable and economic tool in quality control studies of the flex circuits used in hard disk drives. The ability to resolve and image nano scale sized defects in the polymer makes this technique suitable for defect analysis also. UFM gave a better contrast image of the grain structure when compared with the conventional topographic image by AFM. The reason for the better contrast in UFM image is that copper is anisotropic material and the changes in the elastic modulus for different orientations are large thus facilitating the AFM tip to probe the changes in the elastic properties by interacting with the material beneath the tip.

The explanation for the contrast from grain to grain in copper seen in UFM images lies in the crystal structure of the copper. Copper has a Face Centered Cubic (FCC) crystal structure. Copper has three elastic constants,  $C_{11} = 16.84$ ,  $C_{12} = 12.14$ , and  $C_{44} = 7.54$  [25]. Units for elastic constants are  $\text{dyn/cm}^2 \times 10^{-11}$ .  $C_{11}$  is a compressional longitudinal wave and  $C_{12}$  and  $C_{44}$  are transverse shear waves. Anisotropy in cubic crystals is calculated by the ratio of the two shear moduli which is known as Zener ratio or elastic anisotropy factor [26],  $Z$  which is given by

$$Z = 2C_{44} / (C_{11} - C_{12}) \dots\dots\dots (8)$$

The value of Zener ratio for copper is 3.21 which is higher than many materials indicating that copper is highly anisotropic. Usually a Zener value of 1 indicates the material is isotropic. The different crystallography orientation in the copper will exhibit difference in the contrast. For better reliability and optimum current carrying capacity in the copper wires, it is preferred to have only one orientation direction. The high contrast in UFM images indicates that the copper does not have a uniform microstructure and the grains are oriented in different crystallographic orientations. This kind of microstructure may not be suitable for the applications of flex circuits in the hard disk drives. This technique allows for better contrast images of the microstructure of the copper used in the flex circuits without removing the layer of polymer and this technique also could image nano-sized defects present in the polymer layer.

## **CHAPTER 4**

### **IN-SITU IMAGING OF GROWTH OF DELAMINATIONS**

The previous chapter discussed the results of the microstructural analysis on the flex circuits. In addition to the imaging of the microstructure, process-induced defects were also seen in some of the flex circuit samples. Voids in polymer-metal interface or air trapped in the layers of polymer during the manufacturing of the flex circuits are seen as defects in the images obtained using AFM-UFM. The presence of process –induced defects in the flex circuit will seriously limit the life time of the product when it is in actual use. These defects may grow when the flex circuit is subjected to thermal stresses and dynamic flexing actions in a hard disk drive. This chapter discusses the results of simulating the effects of passing the current through a flex circuit sample, and its effects on the growth of the defects at the polymer-copper interface and the polymer.

#### **4.1) Delaminations at Metal/polymer Interface**

In a flex circuit, a copper film is sandwiched between layers of polymer and an adhesive is used to bond those together. The lack of adhesion between the layer of polymer and copper can lead to delaminations in the flex circuit.

Also, excessive moisture absorption by the polymer during the manufacturing can lead to voids and air bubbles in between the layers and can further lead to delaminations. The formation of delaminations at the metal polymer interface in flex circuits can be a cause of concern especially in dynamic applications such as hard disk drives. Although, delaminations are inspected during the manufacturing of the flex circuits, they can still occur while the device is in use due to reasons given above. Study of delamination growth can be used to predict the reliability of the device. Variety of techniques like Scanning Acoustic Microscopy, Scanning Kelvin Probe Microscopy, X-ray photoelectron spectroscopy have been used previously to image delaminations at metal/polymer interface. Most of these studies were carried out to find out delaminations due to electrochemical corrosion. In this study, growth of the delaminations due to passing of current, at the copper/polymer interface of the flex circuits was imaged using AFM/UFM in an in-situ way.

A flex-on suspension (FOS) flex circuit (figure 42) that was used for the microstructural analysis was used in this experiment. To pass current through the flex circuit, wires were micro bonded to the four copper wires of the pre-amplifier part of the flex circuit using thin wires, and at the bottom four wires of the circuit, a copper conducting strip is attached. Two wires were connected to input terminal of a DC constant power supply. The sample, after micro bonding of the wires, was placed on the vacuum stage of the AFM and images were taken while passing a current through the sample by means of DC power supply. The area shown by arrow (as shown in the bottom image of the figure 42) is the region

where the GMR head slider assembly is soldered and hence is chosen for imaging in this experiment.

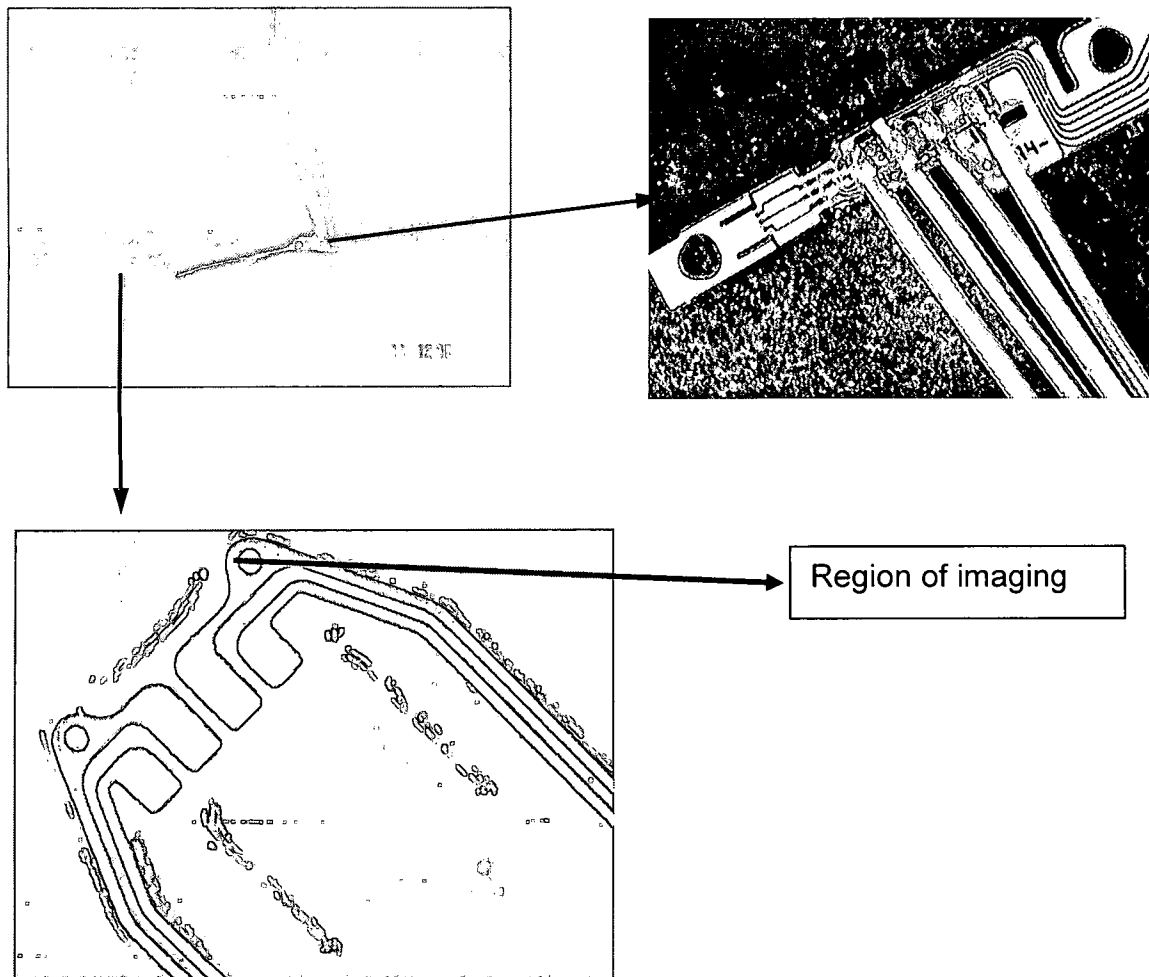


**Figure 42:** Optical microscope image of the flex circuit after micro bonding.

#### 4.2) Results

Figure 43 shows the image taken on the edge of the flex circuit where there is only a polymer layer with no copper present below. The image shows a lot of defects in the polymer layer which may be process-induced or defects present in the raw material of the polymer. These defects may be viewed as



static delaminations present in the flex circuit. These defects under the effect of current and dynamic flexing applications may grow and spread to other regions when the system is in real use.

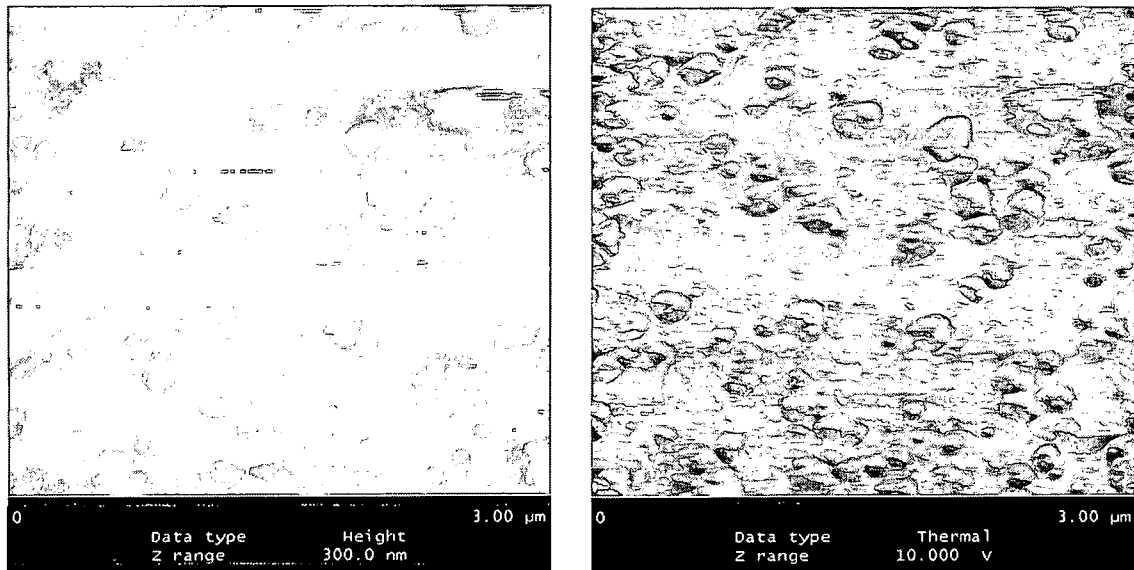


**Figure 43:** Defects in the polymer of the flex circuit .

Initially, a constant current of 50 mA was passed through the sample. Images were obtained in the area chosen for imaging. Image taken after passing current for two hours shows beginning of growth of delaminations in the sample (shown by arrows in the figure 44). A flex circuit is fabricated by laminating copper film and the polymer thin films. During the process of lamination, moisture and air may get trapped in between the layers of copper and polymer. When current is passed through the flex circuit, the trapped air bubbles heats up and bursts, appearing as delaminations at the copper polymer interface.

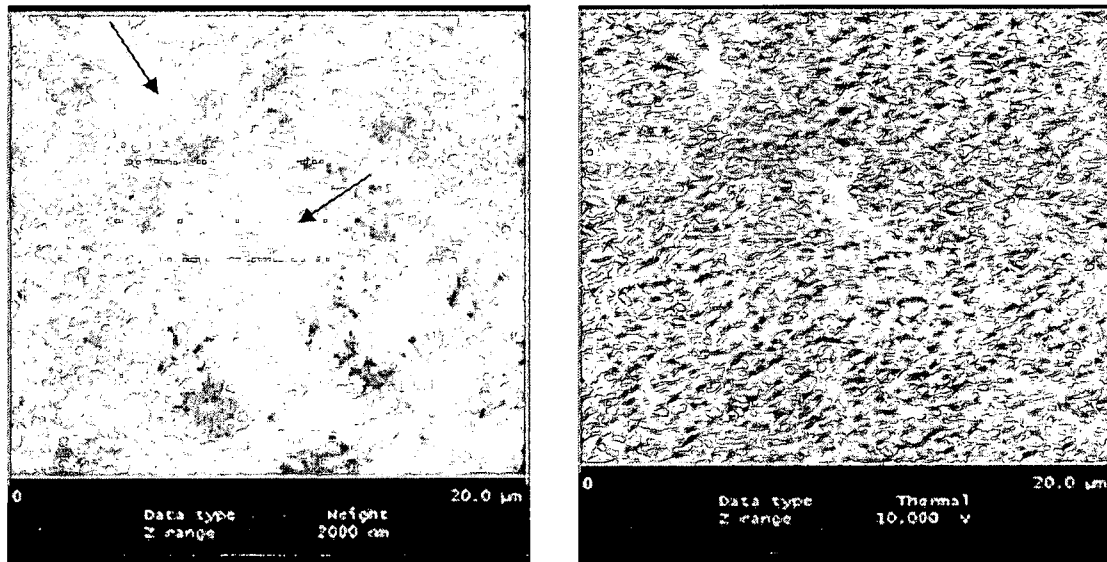


**Figure 44:** Growth of delaminations after two hours of 50 mA current.

After passing 50 mA current for 20 hours, the delaminations in the region began to grow and spread to other regions (figure 45). The image was taken at the same area and same scan size. The areas of the growth of the delaminations are shown by arrows in the figure.

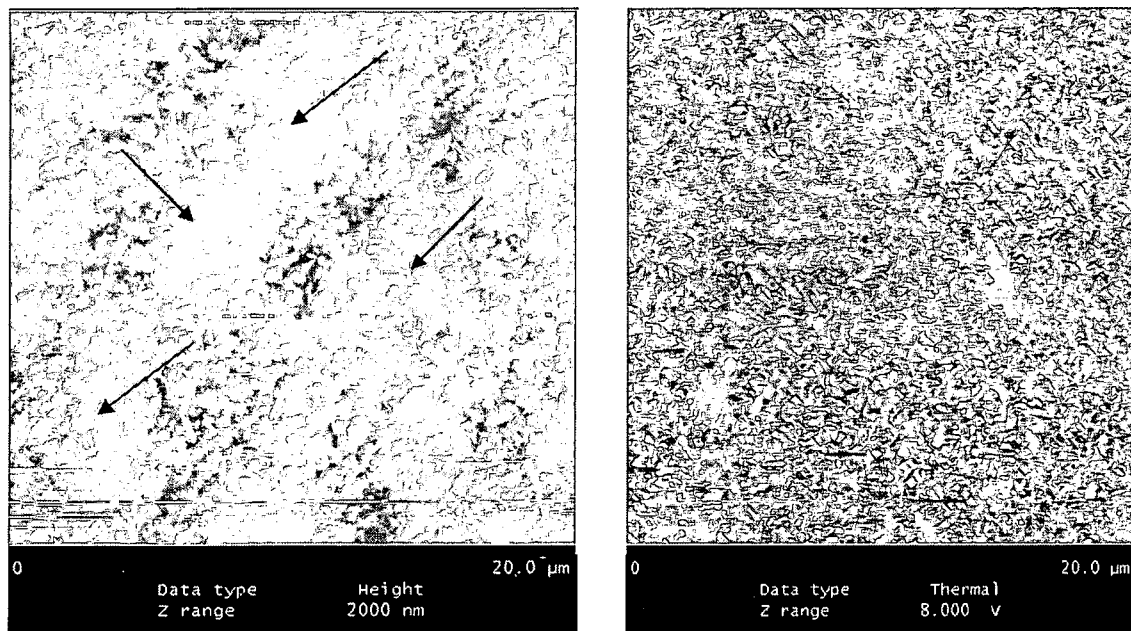


**Figure 45:** Image taken after 20 hours of passing the current (50mA).

The delaminations grew more rapidly after 72 hours of the passage of the 50 mA current (figure 46). The delaminations were growing and extending to other regions of the sample and are seen in the regions which do not have delaminations previously.

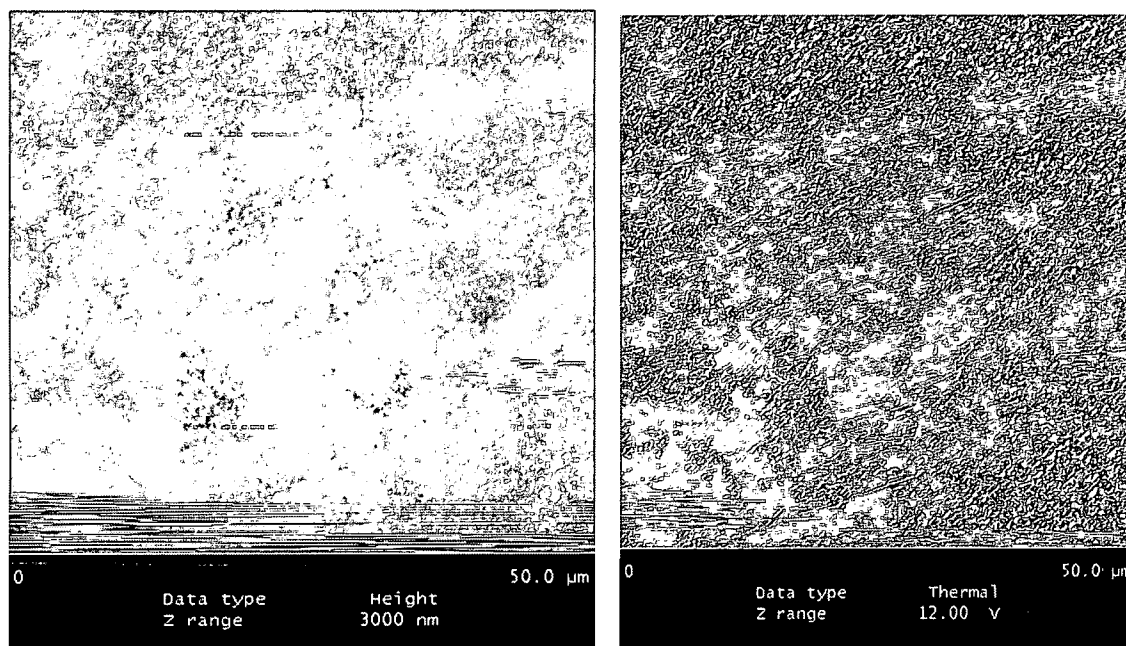


**Figure 46:** Image after 72 hours of 50 mA current.

The current was passed for another 80 hours and no significant growth of delaminations was observed in the flex circuit. After approximately 160 hours of passing the current, the size of the delaminations began to grow with some delaminations as big as 5 microns in length. Figure 47 shows the image obtained at 160 hours of current with a scan size of 10 μm. The UFM image showed some nano-sized particles inside a delamination which may be defects in the polymer.

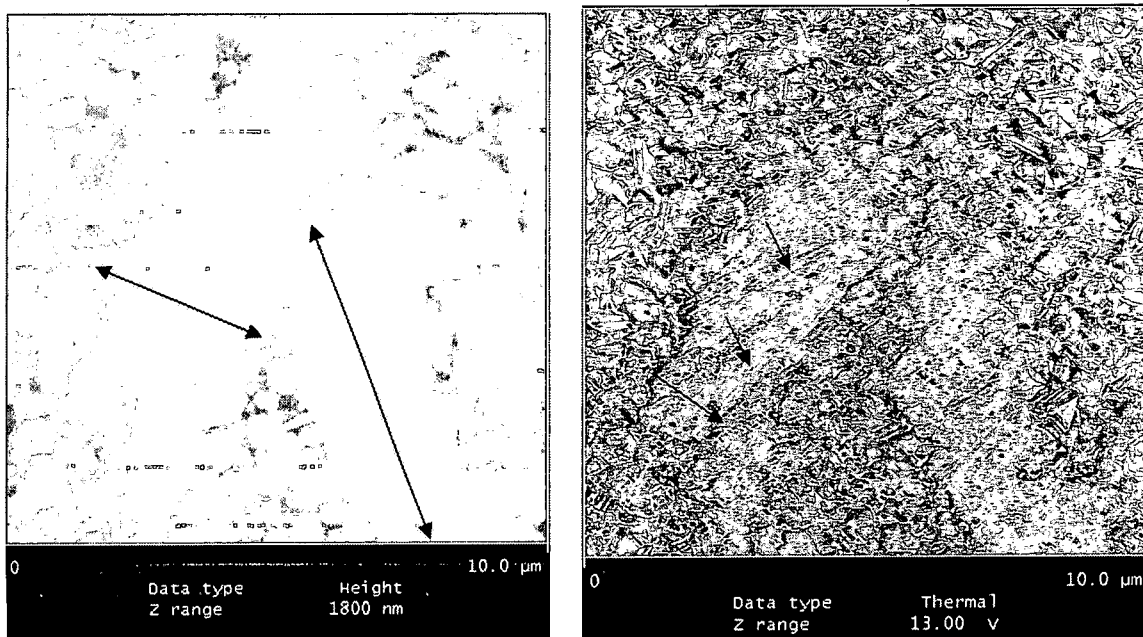


**Figure 47:** Image obtained after 160 hours

The image in the figure 48 shows the magnified region of the delamination of the previous image. This was taken at a scan size of  $1.09\ \mu\text{m}$ . Spherical particles of the size of about 100 nm were seen in this image. They may be defects or inclusions in between the layers of the copper film and the polymer layer. Grain boundaries can also be clearly seen in the UFM image.

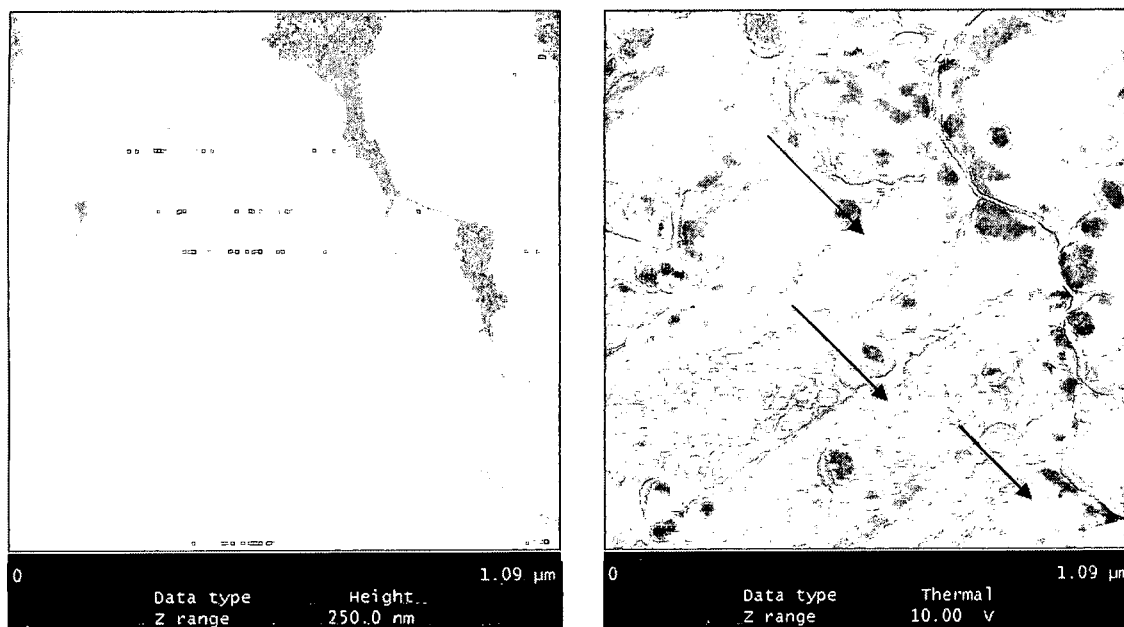


**Figure 48:** Image taken inside a delamination

There was no growth in the delaminations after 160 hours of passing of 50 mA current through the circuit. The current was subsequently increased to 100 mA and after 72 hours of the passing 100 mA current, no significant growth in the delaminations was observed. At this current, another region which was close to the first region was selected for imaging. Figures 49 and 50 shows images taken at this region at different currents and times. The size of the delaminations in this region was similar to that of the first region. No growth of the delaminations was observed even after the current was increased to 800 mA. The image in figure 51 shows the delaminations after passing the 800 mA current. This could be either because the delaminations were stopped at the edge of the copper line or equilibrium was achieved such that there is no driving force for the delaminations to grow further. If more current were passed through the sample, the delaminations would start growing again until the failure of the sample. The failure of the device could be even earlier if we take into account the dynamic

flexing action the circuit will be subjected to in the real time use. The delaminations may grow at a faster rate if the dynamic flexing is also considered.

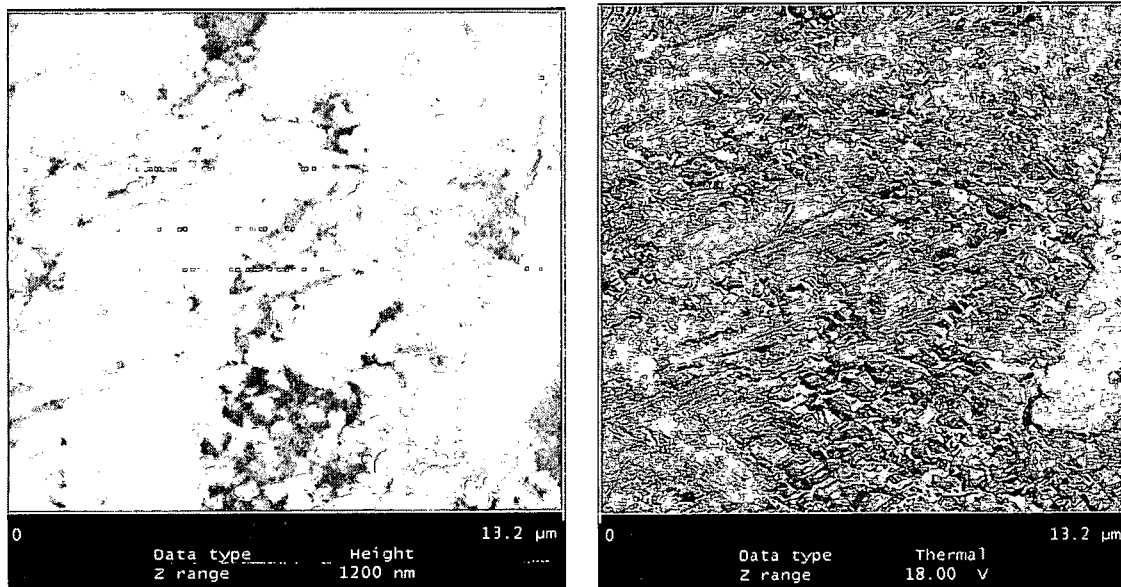


**Figure 49:** Delaminations in region 2

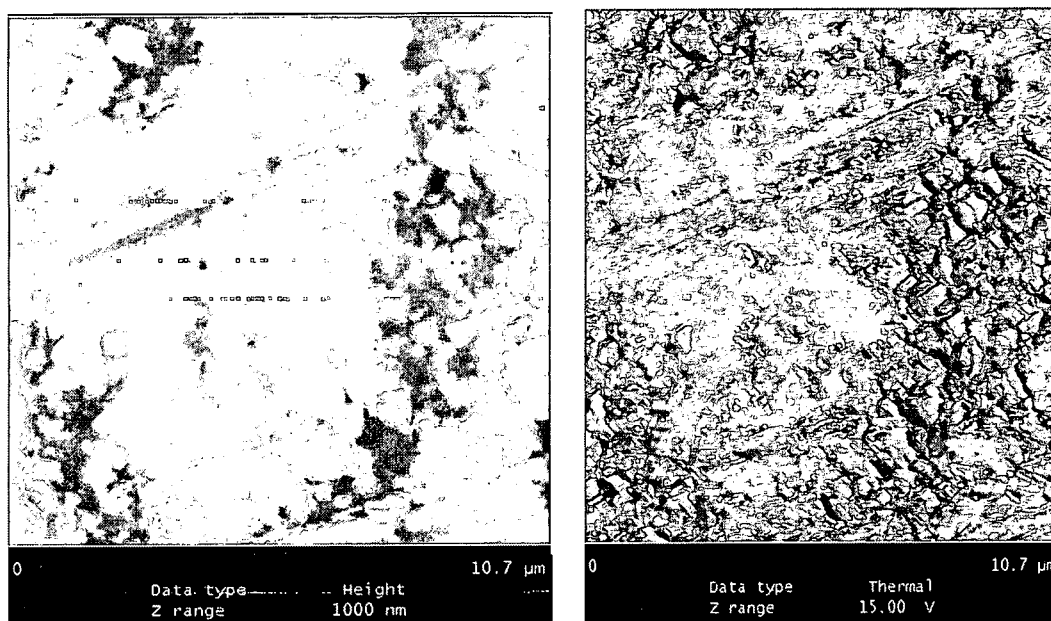


**Figure 50:** Delamination after 48 hours of passing 200 mA (Region 2).

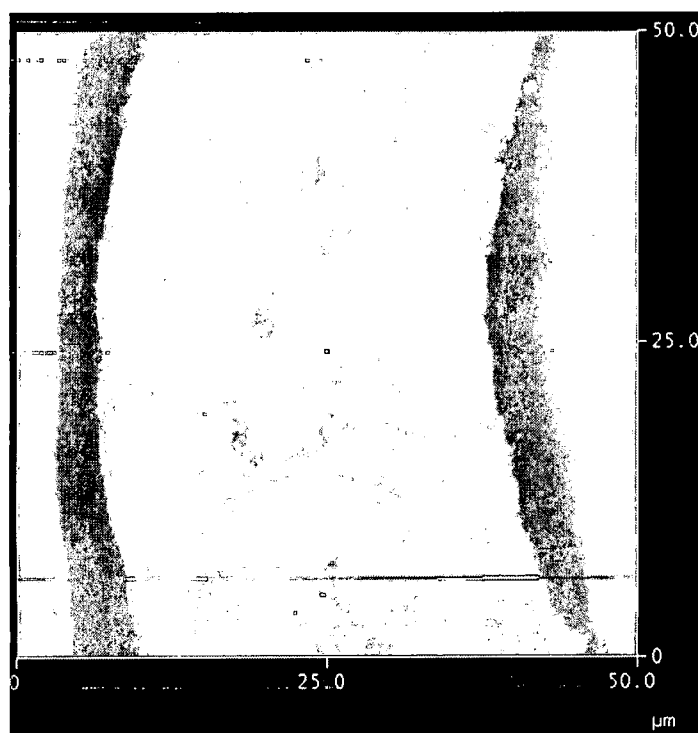


**Figure 51:** Image taken after passing 800 mA current for 24hours.

#### 4.2) Discussion of the Results

The delaminations at the interface of copper and polymer in the flex circuit can be attributed to poor adhesion of the copper and polymer layer, defects in polymer or polymer-metal interface or due to defects at the stage of fabricating the flex circuit. Any of the above factors or a combination of these, can be a driving mechanism for the initiation and growth of the delaminations. The initial appearance of delaminations at the interface of copper/ polymer after passing 50 mA current may be because of the air trapped in between the layers of copper and polymer. Flex circuits are fabricated using roll processing system in which the rolled copper and polymer films, including adhesive, are laminated.

Polyimide, which is extensively used as the base laminate, and cover coats on flex circuits, has a tendency to absorb more moisture [1]. Any moisture absorbed by the polymer during the process of manufacturing the flex circuit, will expand and burst when current is passed through it. These bubbles cannot expand either up or down because of presence of metal and polymer layers thus expanding along the polymer metal interface as delaminations. When the current is passed further, there will be a thermal expansion coefficient mismatch between the copper film and polymer layer. Any defects, voids present in the polymer will try to expand through the layers of copper and polymer but cannot expand and thus are seen as delaminations at the interface of the copper/polymer. The delaminations seen after 20 hours of passing the current and spreading of those delaminations to other regions after 72 hours is due to the presence of defects. The AFM images of the region very clearly show the growth of the delaminations. UFM images which give information about the local changes in the elasticity do not have much contrast essentially because there is no change in the elasticity of the surface because of the growth of the delaminations. These images also show grains of the copper apart from the delaminations along the interface of the copper and polymer.

No significant growth of the delaminations was observed till 160 hours of current was sent through the flex circuit. After 160 hours, the size of the delaminations began to increase even though the delaminations were not spreading to other regions. Images obtained on a smaller scan sizes in the same regions revealed delaminations of the size of approximately 5 microns. UFM



image of the same region also shows nano- sized particles inside a delamination. These particles may be inclusions in the polymer layer or at the interface of copper and polymer. Further magnified scanning image of the inside region of the delamination clearly showed nano- sized defects in the polymer. UFM image of the region clearly shows grain boundaries, along with defects and delaminations with clear contrast. No significant growth of delaminations was observed after the current was increased to 100 mA. At this current, another region near the previous region was selected to image for delaminations. Those images, taken after sending 100 mA of current for 48 hours showed similar delaminations as seen in the first region. The delaminations can be seen all over the region of scanning in this image as these delaminations have already started to grow when the current was passed for initial 72 hours. The growth of the delaminations was not rapid when the current was increased gradually from 100 mA to 800 mA. During the first 160 hours of passing 50 mA current, the delamination growth was faster and was spreading to other regions rapidly. But after the 160 hours, the growth of the delaminations slowed down and not much significant growth was observed even after the current was at 800 mA. Figure 51 shows a 50  $\mu\text{m}$  scan size of the first region of imaging which shows delaminations extending from one edge of the copper line to the other. The lack of growth of the delaminations even when the current is increased may be due to two reasons: a) the delaminations may have reached the edges of the copper line, leaving no room for the delaminations to grow further or b) there was not enough driving force for the delaminations to grow further and may have reached

an equilibrium point. The delaminations could grow if more amount of current is passed for a long periods of time.

With the continued shrinkage of the sizes of the micro-electronic devices, it has become important to understand the phenomenon of delaminations and defects on nano level to better assess the reliability of these devices. The size of the defects is comparable to the width of the copper line of the flex circuits. In a hard disk drive, the flex circuit holds the GMR head slider assembly and thus the reliability of the device depends on the reliability of the flex circuit. The growth of the delaminations was accelerated in this experiment by sending relatively large currents (typically, a hard disk drives has currents less than 50 mA), and the imaging of the delaminations and defects on nano scale serves to assess the reliability of the hard disk drive. This study addressed the effect of the current on the growth of process induced defects in polymer and on the delaminations at the copper polymer interface of the flex circuits. A flex circuit in a hard disk drive also undergoes dynamic flexing action when the arm of the hard disk moves over the magnetic disks to read/write data onto them. The growth of the delaminations which was observed when current was passed through the flex circuit will be more rapid and faster if the dynamic flexing action is also taken into consideration. Proper processing conditions of the fabrication of the flex circuit will reduce the defects in the polymer and copper polymer interface.

## **CHAPTER 5**

### **CONCLUSIONS**

#### **5.1) Summary**

The combination of AFM-UFM has been used to characterize the microstructure of the copper and delaminations at the copper/polymer interface of a flexible circuit in a hard disk drive. Flex circuit is used as an interconnect between the head slider assembly and the arm of the hard disk drive. The microstructure of the copper on the flex circuit is a quality control factor for the hard disk drive manufacturers. The polymer layer underneath the copper has to be removed to obtain the microstructure which is a time consuming and expensive. In this study, the combination of AFM-UFM was successfully used to image the microstructure of the copper through a layer of polymer which was approximately 7  $\mu\text{m}$  thick.

Ultrasonic Force Microscopy, an external modification to the conventional AFM, is a powerful tool for characterizing materials with a better contrast. The contrast in AFM is essentially because of variations in surface topography only. With the advancement of manufacturing techniques, it is now possible to manufacture materials with little variation in topography. In such materials, UFM can resolve nano scale features, which are otherwise buried under the

topography, with better contrast. The contrast is due to the variations in the elasticity of the sample which are sensed by the AFM tip when an ultrasonic wave is passed through the sample attached on a transducer.

The primary goal of this study was to image the microstructure of the copper in the flex circuit through a layer of polymer. Nine flex circuit samples from different manufacturers were used in this study. The microstructure was obtained on each of the sample at different regions and the grains sizes and any variations in the microstructure were investigated in detail on each of the sample. In all the images obtained, UFM images showed great contrast compared to the AFM image. In some of the samples, in addition to the microstructure, defects, voids present in the polymer layers were also clearly imaged. Uniform microstructure was seen in some of the sample where there was no contrast from grain to grain. For micro-electronic devices, it is desirable to have a uniform microstructure of the metal used in it. A uniform microstructure is obtained when all the grains in the metal have same crystallographic orientation. Grains with similar crystallographic orientation have the same elastic modulus and this leads to the lack of contrast in the image. Even though no contrast from grain to grain was seen in some images which show uniform microstructure, the grain boundaries were clearly visible in UFM images showing large contrast at the boundaries. This contrast at the grain boundaries helps to identify the individual grains and perform grain structure analysis. This better contrast in UFM images help to quantitatively evaluate the grain size of the copper which can be difficult if only topographic image was taken. This also helped in identifying defects, voids

clearly at the polymer and at the interface of the polymer and copper which are caused by the processing conditions during the manufacturing of the flex circuits. With the size of the devices constantly decreasing in the micro electronics industry, the defect sizes are approaching the size of the devices. It becomes important to image these nano size defects in order to study the reliability of the device. UFM could image nano sized process induced defects in some of the samples of the flex circuits. The presence of these defects is due to the air trapped in between the polymer layers, or any other defects present in the polymer either in the raw material or during processing of the flex circuit.

The process induced defects seen in some samples, may grow when the flex circuit is subjected to thermal stresses and dynamic flexing action. This study also discussed the effects of passing the current through the flex circuit and imaging the growth of defects. With the passage of the current through the flex circuit, the process induced defects present at the interface of the copper and polymer began to grow and were seen as delaminations in the image. The growth of the delaminations as a function of current and time was discussed. Apart from the imaging of the delaminations at the interface, presence of nano-sized defects was also observed at the interface.

To summarize, the combination of AFM-UFM has been successfully utilized to image the microstructure of the copper through a layer of polymer in flex circuits. Nano scale defects were also imaged along with the microstructure. The growth of the process induced defects and delaminations at the copper

polymer interface as a function of time was investigated and the phenomenon behind the growth was explained.

## REFERENCES

1. Fjelstad, J. *An Engineer's Guide to Flexible Circuit Technology: Materials, Design, Applications, and Manufacturing*, Electrochemical Publications, London, 1997.
2. Bhushan, B. *Tribology and Mechanics of Magnetic Storage Devices*, Springer –Verlag, New York, 1990.
3. Kong, C.W., Yee, H.V. "Design and Characterization of Flexible Circuit for Disk Drive Application", *Ansoft RIDE THE WAVE Technical Seminar*, Singapore, 2001.
4. Li. B., Sullivan.T.D. Lee, T.C., Badami, D. "Reliability Challenges for Copper Interconnects", *Microelectronics Reliability*. Vol. 44, pp365-380. 2004.
5. McCusker, N.D., Gamble, H.S., Armstrong, B.M. "Surface Electromigration in Copper Interconnects", *Microelectronics Reliability*, Vol. 40, pp69-76, 2000.

6. Gladkikh, A., Karpovski, M., Palevski, A., Kaganovskii, Y.S. "Effect of Microstructure on Electromigration Kinetics in Cu Lines", *J.Phys. D: Appl. Phys.*, Vol. 31, pp1626-1629, 1998.
7. Field, D.P., Dornisch, D., Tong, H.H. "Investigating the Microstructure – reliability Relationship in Cu Damascene Lines", *Scripta Materialia*, Vol.45, pp1069-1075, 2001.
8. Nowell, M.M. "Ion Beam Preparation of Passivated Copper Integrated Circuit Structures for Electron Backscatter Diffraction/Orientation Imaging Microscopy Analysis", *Journal of Electronic Materials*, Vol.31, pp23-32, 2002.
9. Besser, P.R., Zschech, E., Blum, W., Winter, D., Ortega, R., Rose, S., Herrick, M., Gall, M., Thrasher, S., Tiner, M., Baker, B., Braeckelman, G., Zhao, L., Simpson, C., Capasso, C., Kawasaki, H., Weitzman, E. "Microstructural Characterization of Inlaid Copper Interconnect Lines", *Journal of Electronic Materials*, Vol. 30, pp 320-330, 2001.
10. Zhang, X., Solak, H., Cerrina, F. "X-ray Microdiffraction Study of Cu Interconnects", *Applied Physics Letters*, Vol.76, pp315-317, 2000.



11. Hasegawa, M., Hirai, Y. "Microscopic Observation of Cu Damascene Interconnects Grains Using X-ray Microbeam", *Journal of Applied Physics*, Vol.90, pp 2792-2795, 2001.
12. Stratmann, M., Leng, A., Furbeth, W., Streckel, H., Gehmecker, H., Grobe-Brinkhaus, K.H. "The Scanning Kelvin Probe: A New Technique for the In-situ Analysis of Delamination of Organic Coatings", *Progress in Organic Coatings*, Vol. 27, pp261-267, 1996.
13. Nazarov, A.P., Theierry, O. "Scanning Kelvin Probe Study of Metal/polymer Interfaces", *Electrochimica Acta*, Vol.49, pp 2955-2964, 2004.
14. Rohwerder, M., Hornung, E., Stratmann, M. "Microscopic Aspects of Electro-chemical Delamination: An SKPFM Study" *Electrochimica Acta*, Vol. 48, pp1235-1243, 2003.
15. Hummelgen, I.A., Roman, L.S., Nart, F.C., Peres, L.O., de Sa, E.L. "Polymer and Polymer Metal Interface Characterization via Fowler-Nordheim Tunneling Measurements", *Applied Physics Letters*, Vol.68, pp3194-3196, 1996.

16. Boerio, F.J., Hong, P.P., Tsai, W.H., Young, J.T. "Non-destructive Characterization of Polymer/metal Interfaces Using Surface Enhanced Raman Scattering", *Surface and Interface Analysis*, Vol. 17, pp448-456, 1991.
17. Digital Instruments, Inc. Santa Barbara, CA. "Dimensions™ 3000 Scanning Probe Microscope, Instruction Manual,"1996.
18. Binnig, G., Quate, C.F., Gerber, C.H. "Atomic Force Microscope", *Physical Review Letters*, Vol. 56, pp930-933, 1986.
19. Bhushan, B. *Handbook of Nano technology*, Springer-Verlag, New York, 2004.
20. Prater, C.B., Maivald, P.G., Kjoller, K.J., Heaton, M.G. "Probing Nano-scale Forces with the Atomic Force Microscope", Digital Instruments Application Notes.
21. Yamanaka, K. "Ultrasonic Force Microscopy", *MRS Bulletin*, Vol.21, Oct., 1996.

R00252277

22. Burnham, N., Kulik, A.J., Gremaud, G., Gallo, P.J., Oulevey, F. "Scanning Local Acceleration Microscopy", *Journal of Vacuum Science and Technology*, Vol.14, pp794-799, 1995.
23. Rabe, U., and Arnold. W. "Acoustic Microscopy by Atomic Force Microscopy", *Applied Physics Letters*, Vol.64, pp1493-1495, 1994.
24. Schumaker, E.J., Shen, L., Ruddell, M., Sathish, S., Murray, P.T. "Ultrasonic Force Microscopic Characterization of Nano-sized Copper Particles" *Nanophase and Nanocomposite Materials III. Symposium (Materials Research Society) Proceedings* Vol.581, pp473-477, 2000.
25. Truell, R., Elbaum, C., Chick, B. *Ultrasonic Methods in Solid State Physics*, Academic Press, New York, pp370, 1969.
26. Green, D.J. *An Introduction to the Mechanical Properties of Ceramics*, Cambridge University Press, New York, 1998.